Journal of Earthquake Engineering
Publication details, including instructions for authors and subscription information:
http://www.tandfonline.com/loi/ueqe20

SOIL AND TOPOGRAPHIC AMPLIFICATION ON CANYON BANKS AND THE 1999 ATHENS EARTHQUAKE

D. ASSIMAKI [a] & G. GAZETAS [a]

[a] Graduate Research Assistant, Massachusetts Institute of Technology, USA

[b] Professor, National Technical University of Athens, Athens, Greece

Version of record first published: 03 Jun 2008.

To cite this article: D. ASSIMAKI & G. GAZETAS (2004): SOIL AND TOPOGRAPHIC AMPLIFICATION ON CANYON BANKS AND THE 1999 ATHENS EARTHQUAKE, Journal of Earthquake Engineering, 8:1, 1-43

To link to this article: http://dx.doi.org/10.1080/13632460409350479

Journal of Earthquake Engineering, Vol. 8, No. 1 (2004) 1–43

Imperial College Press
www.icpress.co.uk

SOIL AND TOPOGRAPHIC AMPLIFICATION ON CANYON BANKS AND THE 1999 ATHENS EARTHQUAKE

D. ASSIMAKI
Graduate Research Assistant, Massachusetts Institute of Technology, USA

G. GAZETAS
Professor, National Technical University of Athens, Athens, Greece

Received 26 August 2002
Revised 23 May 2003
Accepted 1 July 2003

A time-domain parametric study for the seismic response of a region located on the eastern bank of the Kifisos river canyon is performed to evaluate the significance of topography and soil effects on the seismic response of slopes. This region experienced unexpectedly heavy damage during the 7 September 1999 M_s 5.9 earthquake. Two-dimensional finite-element and spectral-element analyses are conducted using Ricker wavelets of various central frequencies as horizontal and vertical base excitation. The significance of a layered soil profile and the frequency content of the input motion, the emergence of "parasitic" acceleration components, and the effect of the angle of incidence on the amplification of the incoming waves are all discussed in detail. It is shown that the presence of a surface soil layer significantly affects the amplification pattern. The so-called Topographic Aggravation Factor (defined as the 2D/1D Fourier spectral ratio) achieves its maximum value very near the crest, in function of the frequency content of the excitation. For the particular soil conditions and geometry analysed, vertically propagating SV waves incite at about the *critical* angle, resulting in the highest topographic amplification.

Keywords: Site effects; topography; amplification; stratigraphy; 1999 Athens Earthquake; 2D wave propagation.

1. Introduction

It has long been recognised that the destructiveness of ground shaking during earthquakes is affected significantly by "*local soil conditions*", a term referring to the thickness and stiffness of the soil layers, from surface to bedrock, at a particular site. Thus, observed wide differences in damage from site to site within a city have often been convincingly attributed to differences between the underlying soil deposits. A few classical examples: the non-uniform distribution of damage in Tokyo during the 1923 Kanto Earthquake [Ohsaki, 1969]; in Caracas during the 1967 Venezuelan Earthquake [Seed *et al.*, 1972]; in Bucharest during the 1977 Vranehla Earthquake [Tezcan *et al.*, 1979]; in Mexico City during the Earthquakes of 1957 and especially of 1985 [Rosenblueth, 1960; Seed and Romo, 1987]; in San Francisco and Oakland

during the 1989 Loma Prieta Earthquake [Housner, 1990]; in Kobe during the 1995 Earthquake [*Special Issue of* Soil and Foundations, 1996]; and in Adapazari during the Kocaeli Earthquake [*Special Issue of* Earthquake Spectra, 2000].

Acceleration signals recorded in the last three decades revealed in many cases that the subsoil characteristics had appreciably influenced the amplitude level, the frequency composition, and the duration of shaking. The term "soil amplification" has been coined to describe the "filtering" which seismic waves undergo as they pass through the soil, and which tends to reinforce certain harmonic components of the incoming waves. On the other hand, soil "filtering" can also depress those harmonic components of the incident seismic wave whose frequencies exceed substantially the natural frequencies of the soil deposit. "De-amplification" of the shaking is thus possible. Well-documented case histories involving a very significant recorded de-amplification of seismic motion by a very soft layer have been presented, among others, by Seed and Idriss [1970], and Gazetas *et al.* [1990].

The presence of a strong topographic relief (such as a hill, a ridge, a canyon, a cliff, or a slope) can also have an effect on the intensity and frequency composition of ground shaking during earthquakes.

Scattering or diffraction of the incident seismic waves can in such cases generate large amplification of ground shaking over short distances. However, the phenomenon is more complicated to analyse than is "soil amplification", due to its truly two- or three-dimensional nature. Thus it has received less attention, and it has not been incorporated in seismic codes.

Evidence from destructive earthquakes shows that damaging effects tend to increase where steep relief or complicated topography is present. In the recent past, there have been numerous cases of recorded motions and observed earthquake damage pointing towards amplification due to local site conditions as an important effect. Prompted by such observations, a considerable amount of work has been done to analyse and predict these effects. Many authors have studied the problem of scattering/diffraction of seismic waves by topographical "irregularities", usually under simplified assumptions of elastic soil behaviour, two-dimensional geometry of the analysed configurations, vertically propagating incident waves, and harmonic steady-state excitation.

One of the first numerical studies on the effect of topography on seismic response was carried out by Boore [1972], using finite differences. Subsequent studies were conducted using finite elements [Smith, 1975], boundary elements [Sanchez-Sesma *et al.*, 1982], and discrete wave number methods [Bard, 1982]. According to the review article by Geli *et al.* [1988], most analyses refer to the case of a two-dimensional ridge on the surface of a homogeneous half-space and have given consistent results, namely maximum amplification of acceleration at the crest of two over the horizontal surface of an otherwise identical medium. However these results considerably underestimate amplification values observed in the field during microtremors (earthquake weak motions), which have been reported as high as 10.

Geli *et al.* [1988] successively analysed a more detailed configuration consisting of a layered profile and introduced nearby ridge effects, arriving at results similar to those of the aforementioned researchers. In addition, they concluded that the presence of surface topography irregularities might have greater effect on site response than soil layering and "flexibility".

It should be noted however that most research studies performed on topography effects have thus far focused on ridge type surface irregularities. According to Ashford *et al.* [1997], whereas some of the procedures and concepts developed for the analysis of ridges may also be extended to slope topographies, the semi-infinite nature of the soil profile in the horizontal direction behind the slope crest and the potential of soil amplification of the motion in the 1-Dimensional sense can cause significant differences between the response of soil slopes and ridges.

Focusing specifically on the seismic response of soil slopes, Idriss and Seed [1967], Kovacs *et al.* [1971], May [1980], and Sitar and Clough [1983] showed analytically and with case studies that even if the motion were amplified in the vicinity of the crest, the natural period of the 1D soil column behind the crest was responsible for larger amplification of the input motion than the amplification due to slope geometry, in contrast to Geli *et al.* [1988].

2. Evidence of Topographic Effects: Literature Review

It has been often reported after destructive earthquakes that buildings located at the tops of hills, ridges and canyons, suffer more intensive damage than those located at the base: examples of such observations may be found in Boore 1972 (San Fernando Earthquake, 1971), Levret *et al.* 1986 (Lambesc Earthquake, France 1909), Brambati *et al.* 1980 (Friuli Earthquake, Italy 1976), Siro 1982 (Irpinia Earthquake, Italy 1980), Celebi 1987 (Chile Earthquake, 1985), Kawase and Aki 1990 (Whittier Narrows Earthquake, 1987), and Restrepo and Cowan 2000 (Armenia or "Eje-Cafetero" Colombia Earthquake, 1998). Recent earthquakes in Greece (Kozani, 1995 and Athens, 1999) brought additional evidence of severe damage in structures built on hilltops or close to steep slopes.

There is also very strong instrumental evidence that surface topography affects the amplitude and frequency contents of the motion: reviews of such instrumental studies and results can be found in Geli *et al.* [1988], Faccioli [1991] and Finn and Liam [1991]. A strong recorded topographic effect was presented first in Bard and Meneroud [1982], and verified by Nechtschein *et al.* [1995], for a steep site in Southern Alps, with a crest to base spectral ratio as high as 20, but within a narrow frequency band around 5 Hz. Another well-known case history of recorded evidence of topographic amplification comes from the strong motion recordings in Tarzana station during the Northridge, California 1994 earthquake, for which spectral amplification was of the order of 5 in the vicinity of 3 Hz [Celebi, 1995; Bouchon and Barker, 1996]. Similar observations during weak seismic shaking were

recently reported from Greece [Chavez-Garcia *et al.*, 1996; Lebrun *et al.*, 1999]. However, the number of instrumental studies on topographic effects is very limited and therefore it is not possible to derive reliable conclusions of a general nature.

Theoretical models predict a systematic amplification of seismic motion at ridge crests, and more generally, over convex topographies such as cliffs. Correspondingly, they also predict de-amplification over concave topographic features such as valleys and the base of hills. The extent of these effects has been proved to be rather sensitive to the characteristics of the incident wavefield (wave type, incident and azimuth angles). Theory also predicts complex amplification and de-amplification patterns on hill slopes, resulting in significant differential motions. In particular, according to Bard [1999], these effects are related to three physical phenomena:

(i) The sensitivity of the surface motion to the incidence angle, which is especially large for SV waves around the critical angle. The slope angle thus produces significant variations in surface motions. Kawase and Aki [1990] suggested this effect as a contributing cause to the peculiar damage distribution observed on a mild slope during the Whittier Narrows, California earthquake of 1987.

(ii) The focusing or defocusing of seismic waves reflected along the topographic surface. Sanchez-Sesma [1990] provided an insight into this effect through the example of a wedge-shaped medium. Up to now, there has not been adequate instrumental proof of such focusing/defocusing effects in *strong* seismic shaking, since the few available in the world 3D seismological arrays on a topographic feature are still of a young age.

(iii) The diffraction of body and surface waves which propagate downwards and outwards from the topographic features, and lead to interference patterns between the direct and diffracted waves. However, these diffracted waves generally have smaller amplitudes on the surface than the direct body waves, at least for smooth natural topographies. Such interference patterns consistently predicted by theory have been reported by Pedersen *et al.* [1994] from semi-dense array recordings in Greece, where the amplitude of the outwardly going waves was shown to be about one-fifth of that of the primary wave.

The effects of a convex topographic irregularity, such as a cliff or a ridge, are among the most frequently encountered and thereby studied, both numerically and theoretically. In such a configuration, two free-field locations exist, in contrast to the ridge-type topography: behind the cliff crest and at the cliff toe, where two-dimensional topography effects play negligible role in the resulting surface response (see Fig. 1). In the present study, the ratio of the motion near the top of the cliff to the motion at distance $x = 300$ m (selected invariably for all studied cases) is used as a measure of the two-dimensional amplification of motion ($a_{\max}/a_{ffc}$).

For a harmonic excitation, the main parameters affecting the response are:

- the height H and the slope angle i of the cliff, and
- the wavelength λ, the angle of incidence β, and nature of the incident waves.

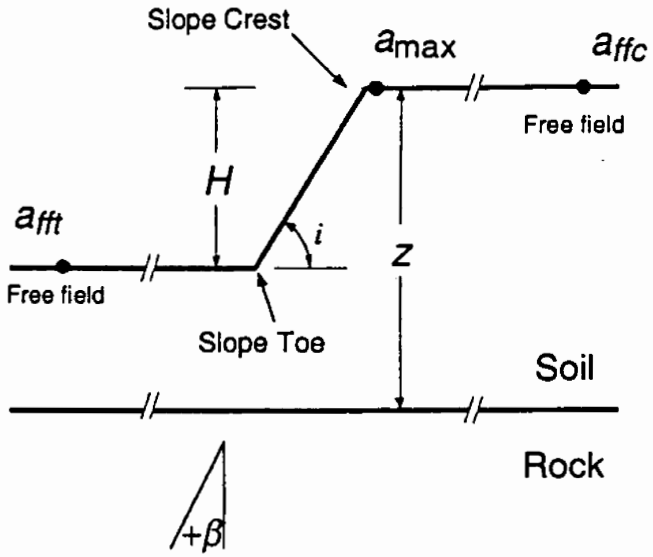

Fig. 1. Definition of dimensions and symbols for the study of cliff topography effects, with the two free-field locations [after Ashford and Sitar, 1997].

Other parameters playing important role are the two- or three-dimensional nature of the configuration and the stratigraphy of the profile (shear wave velocity variation with depth).

In what follows, the effect of the aforementioned parameters on the surface ground motion will be reviewed in detail utilising published theoretical and experimental evidence.

2.1. *Effect of nature of incident waves*

SH waves have been studied more frequently [i.e. Ohtsuki and Harumi, 1983], as reflection and diffraction of SH waves does not generate other wave types [e.g. P, SV or Rayleigh] — in contrast with P or SV waves. In general however, it has been shown that the amplification of SV waves is usually higher than that of the SH waves. In particular, according to Ashford and Sitar [1997], a vertical cliff subjected to vertically propagating SH waves resulted in a maximum amplification at the surface of the order of 1.25 (with respect to the free-field), whereas for the same configuration, a maximum amplification of the order of 1.5 was observed in the case of vertically propagating SV waves. Qualitatively, the pattern of distribution of soil amplification and de-amplification of seismic motion as a function of the distance from the cliff, is similar for SH and SV waves.

Diffraction of incident SV waves at the edges and on the surface of a slope produces additional wave types, such as Rayleigh waves. According to Ohtsuki and Harumi [1983], Rayleigh waves produced at the toe of the slope propagate upwards along the slope and the horizontal surface of the cliff, preceded by Rayleigh waves resulting from the incidence of SV waves at the crest of the slope. Boore *et al.* [1981] predict dispersive Rayleigh waves with amplitudes approximately 40% of the amplitude of the corresponding incident wave (P or SV) at the free-field surface, for

wavelengths λ somewhat larger than the height H of the vertical slope. Similarly Ohtsuki and Harumi [1983] show that the amplitude of Rayleigh waves at the horizontal surface behind the slope crest is 35% of the amplitude of the incident waves at the free field surface. Therefore, there is a zone in the vicinity of the slope, where high amplification of the incident seismic motion occurs due to the combination of primary SV and diffracted Rayleigh waves.

2.2. *Effect of direction of the incident waves*

The direction of propagation of the incoming seismic waves can be described by the angle of incidence β (Fig. 1) and the azimuth (angle with respect to the North direction on the horizontal plane). Restricting our attention to 2D configurations, we discuss only the effect of β.

Ashford and Sitar [1997] studied the effect of β for a vertical slope, performing parametric studies in the frequency domain and in the time domain using three real acceleration time histories. Their study was limited to angles smaller than the critical angle, β_{cr}. When the angle of incidence of the propagating S-wavefield coincides with the critical angle, a transformation takes place, and a single P-wave arises and propagates along the slope.

It was concluded that a large spatial variation of surface motion arises for nonzero angles of incidence. In particular for SH waves and a vertical slope, the horizontal response at the crest might be of the order of 25% and 100% higher than the corresponding free field motion for $\beta = 0°$ and $\beta = -30°$ respectively. Results similar to those for SH waves were obtained for the horizontal component of the SV wave, except that now the amplification is much greater (by a factor exceeding 2) for waves travelling into the slope (i.e. $\beta < 0$), and there is less attenuation for waves travelling away from the slope. This dependency on the direction of propagation for horizontal (but not vertical) response is in general agreement with results of Pedersen *et al.* [1994]. There is a notable increase in the vertical response due to SV waves at low frequencies, which increases with incident angle, independently of the direction of propagation, due to wave splitting on the free surface rather than energy focusing at the slope crest.

From site-specific analyses, it was concluded that even though topographic *amplification* ratio is greater for inclined waves, the absolute magnitude of acceleration at the crest (both horizontal and vertical) is generally greatest for the case of vertically propagating waves. Therefore, the simplification of a vertical incidence is adequate.

2.3. *Effect of slope inclination*

Ashford and Sitar [1997] studied the effect of the cliff slope on the response of the crest to vertically propagating SV and SH waves. It appears that as the slope becomes less steep, the magnitude of amplification at the first peak decreases by

25% to about 15%, but this trend is reversed at higher frequencies: a mild 45° slope experiences about 50% higher amplification than the vertical slope.

Boore *et al.* [1981] studied the effect of a cliff slope to the dispersion of the incident waves. For incident S-waves, there is higher dispersion at the crest when compared to the dispersion at the toe, both for vertical slopes as well as for 45° slope angles. For incident P-waves, the dispersion is higher for vertical slopes than for 45° slope angles, whilst higher dispersion is observed at the toe of the cliff. Finally, for both slope angles (45° and 90°), it is observed that dispersion of S-waves results to Rayleigh waves with broader bandwidth than Rayleigh waves from P-wave dispersion.

Ohtsuki and Harumi [1983] studied the effects of the slope angle for the case where the horizontal surface at the toe of the slope is covered with a soft surface layer. It was noted that for two different slope angles analysed, the horizontal response in the vicinity of the slope toe was practically invariant.

2.4. *Spatial variation of ground motion along the bank of a canyon*

The distance from the crest of the cliff where the surface response is no longer affected by the presence of the topographic irregularity (i.e. the free-field) is a function of the wavelength, rather than a constant.

Ohtsuki and Harumi [1983] show dimensionless plots of the spatial distribution of the response along the free surface, for a cliff subjected to vertically propagating SV waves, with $h/\lambda = 0.5$, 0.25 and slope inclination of $i = 63.44°$, as well as for a cliff covered at its foot by a soft layer.

The effects of ridge type topography on the spatial distribution along the free surface could be also qualitatively evaluated by studying the two-dimensional scattering of the incident waves by canyons. Trifunac [1973] and Wong and Trifunac [1974] studied the two-dimensional scattering and diffraction of plane SH waves by a semi-cylindrical and by a semi-elliptical canyon respectively. Surface amplifications inside and near the canyon were found to depend on two key parameters: the angle of incidence and the ratio of the canyon width to the wavelength of incident SH waves. Results of surface displacement amplitudes evaluated for shallow canyons (where the interaction of scattered wave fields due to the simultaneous presence of two ridges could be neglected) could be also used to assess the displacement pattern along the surface behind the crest of a ridge. Sanchez-Sésma [1987] also studied the two-dimensional scattering of SH waves by a triangular canyon. Typical results are shown in Fig. 2 for the normalised amplitudes on the surface as a function of the canyon height, h. For shallow canyons, the results approach the response of ridges studied herein.

Even if there is no established criterion for the location away from the slope where the free-field motion is retrieved, results of studies performed show that this distance is strongly dependent on the geometry of the configuration, the frequency of the input motion, and the soil material damping. In the present study, the

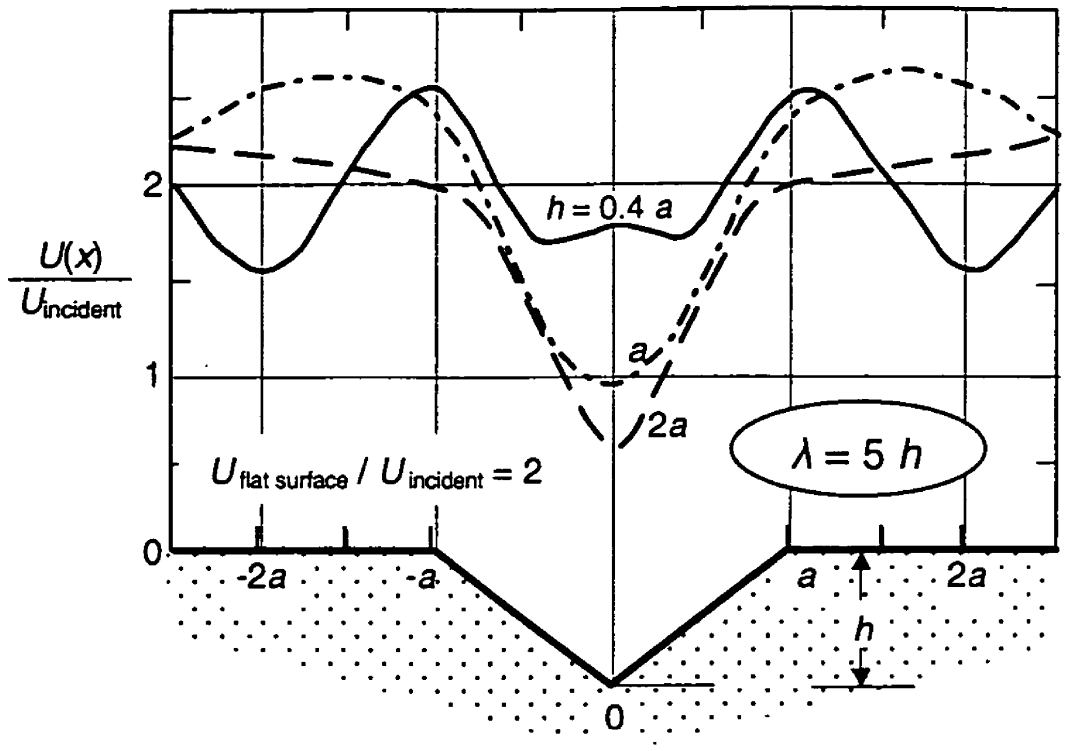

Fig. 2. Displacement amplitudes on the surface of a triangular canyon for different canyon heights h and normalised frequency $\lambda/h = 0.2$, incidence of SH waves (modified from Sanchez-Sésma, 1987).

free-field motion has been invariably defined at a distance $x = 300$ m from the crest, even if topography effects were practically negligible for $x > 150$ m (≈ 3.5 H) for most of the cases studied. Since however soil nonlinearity has been taken into account by means of the equivalent linear method, this distance should be mainly considered as a lower bound.

2.5. *Effect of the frequency content of base excitation*

Topography effects are very significant for wavelengths comparable to the geometric characteristics of the irregularity, whereas they are considered negligible for very low frequencies, i.e. very long wavelengths [Butchbinder and Haddon, 1990; Ohtsuki and Harumi, 1983; Aki, 1988; Ashford *et al.*, 1997]. In the case of the cliff, the dimensionless frequency at which the first peak of the response is observed is considered to be of utmost importance.

For hill or canyon it was observed that diffractions at the slope surface play a major role on the modulation of the surface response, the effect of which depends on the ratio H/λ. As mentioned in a preceding section, amplification is more apparent for SH waves with direction $\beta < 0$, and the first peak in the amplification spectrum is observed at $H/\lambda = 0.2$. On the contrary, for SH waves with direction $\beta > 0$, there is negligible amplification for $H/\lambda < 0.2$, whereas de-amplification is observed for higher values [Ashford and Sitar, 1997]. For the case of vertical incidence in particular, amplification peaks are observed at values $H/\lambda = 0.2$ and $H/\lambda = 0.7$,

very close to the values of the resonant frequencies of the soil column behind the crest of the slope ($H/\lambda = 0.25$ and $H/\lambda = 0.75$ respectively).

For the case of SV waves, the horizontal component of the motion as a function of the dimensionless frequency shows similar behaviour with the corresponding of the SH waves, with the peaks being observed at $H/\lambda = 0.2$ and $H/\lambda \approx 1$. For the vertical component, there is a monotonic increase of the maximum value as a function of the dimensionless frequency, whereas for very low frequencies ($H/\lambda < 0.05$), the vertical component becomes almost zero.

2.6. *Other parameters*

In the preceding sections, the main parameters affecting the topographic amplification or de-amplification of seismic motion have been analysed. There exist however numerous cases, where the observed amplifications are significantly larger than the theoretical predictions obtained from sophisticated, two- or three-dimensional models [Bouchon *et al.*, 1995; Ashford *et al.*, 1997]. Therefore, the effects of *secondary* parameters on the modulation of the surface response in the vicinity of topographic irregularities need to be also taken into account.

- ***Soil stratigraphy***
  The role of the soil stratigraphy on the surface response of two- or three-dimensional topographic features may be important. In particular, strong amplification is observed when the incoming wavefield is rich in frequencies close to the natural frequency of the soil layer behind the crest.

  Ashford *et al.* [1997] expressed the amplification of the input motion as a function of the natural frequency of the soil column beyond the crest. A vertically stepped layer over a halfspace was used in the analyses, and the material properties of the underlying halfspace were selected such that the resulting impedance would be three times the impedance of the stepped layer. The natural frequency of the soil column behind the crest was successively controlled in the parametric studies by varying the thickness of the layer. Results of the aforementioned study show that the natural frequency of the site had a greater effect on surface amplification than does the topography itself, for high levels of impedance ratio.

  In the view of the above studies, it is clear that the relative importance of topography and soil flexibility in the amplification of seismic motion behind slope surface irregularities is still an unsettled issue, and site specific investigation is necessary to assess the resulting response, irrespective of the prescribed seismic input motion.

- ***Material damping***
  Ashford and Sitar [1997] studied the effect of material damping ratio on the response. In particular, they performed parametric studies for low values of material damping ($\xi = 1\%$ and $\xi = 5\%$), and studied the effects on the slope crest response. In general, the normalised response (with respect to the

free-field motion) decreases as material damping increases. The same holds for the absolute response at the crest, yet in this case the decrease is more apparent, even for small changes in the damping ratio.

Finally, material damping also affects the extent of the area where the response is governed by the topographic irregularity, which becomes more confined in the vicinity of the slope as the nonlinear behaviour (and therefore material damping) increases, i.e. for high intensity seismic input.

2.7. *Conclusions of the review*

Based on the conclusions of the studies revisited in the preceding sections, it can be readily seen that the factors, which affect the extent and area of influence of topographic irregularities cannot be easily isolated.

As a general rule for incident harmonic SH waves, the maximum steady-state horizontal acceleration at the slope crest takes values about twice the acceleration at the free field beyond the crest, for wavelengths of the same order of magnitude as the geometrical characteristics of the cliff. Along the slope surface, there exists both amplification and de-amplification of the input motion. A similar behaviour governs the response in the case of incident SV waves, with the maximum amplification values being in general slightly higher.

Conclusions drawn by Geli *et al.* [1988], based on the compilation of instrumental and theoretical results, and revisited by Bard [1999], can be summarised in the following:

(i) there is a qualitative agreement between theory and observations about the existence of seismic motion amplification at ridges and mountain tops, and de-amplification at the base of hills. The amplification is generally larger for horizontal components (roughly corresponding to S-motion) than for the vertical component (mostly P-motion).

(ii) the observed or computed amplification seems very roughly related to the "sharpness" of the topography: the steeper the average slope, the higher the top amplification.

(iii) this amplification (or de-amplification) phenomenon is frequency-dependent. There is a satisfactory qualitative agreement between instrumental observations and theoretical results for the relation between geometrical and mechanical characteristics of a given topography and the frequency range where amplification is significant: the maximum effects correspond to wavelengths comparable to the horizontal dimension of the topographic feature.

(iv) However, from a *quantitative* viewpoint, the situation is somewhat confusing, as already stated in Geli *et al.* [1988]. There exist cases where field measurements exhibit only very weak amplifications at ridge crests, and fit very well the numerical results [Rogers *et al.*, 1974]. However, there also exist numerous cases where the observed amplifications are significantly larger than the theoretical predictions obtained from sophisticated, two- or three-dimensional models [Bouchon *et al.*, 1995]. There are numerous observations of spectral

amplifications larger than 10, but only two predictions of such amplitude by numerical models. This confusing situation has been confirmed by some recent instrumental studies in Greece, California and the French Alps [Pedersen *et al.*, 1994; Nechtschein *et al.*, 1995; Bouchon and Barker, 1996; Leburn *et al.*, 1999]. In the first case, only weak amplifications are reported at ridge crest that fit very well the numerical results, in agreement with a few previous observations [Rogers *et al.*, 1974; Tucker *et al.*, 1984]. Large amplifications are also reported for the other sites, including very rapid variations of ground motion amplitude along the slope: over horizontal distances smaller than 200 m, and altitude differences of a few tens of meters, there may exist a difference of about one order of magnitude, in qualitative agreement with previous damage observations at the same sites. This latter case also provided a good example of motion deamplification at valley bottom, which leads to very high values (several tens) for the crest/base spectral ratio.

The focusing of seismic energy in convex topographies, as predicted by theoretical models, certainly plays a significant role in observed amplification effects. It does not seem however to be the only physical phenomenon involved. For this reason, controlled instrumental studies should be performed with dense arrays and detailed geotechnical surveys, if advances in the understanding of surface topography effects are to be made.

A case study from the Athens 7 September 1999 Earthquake, where the simultaneous effect of topography, soil profile, and input motion characteristics resulted in the amplification of motion on the banks of a canyon is analysed in the sequel. Parametric studies are performed in an attempt to understand the role of key parameters that affected the response and inflicted the heavy damage at the structures of the analysed site.

3. The Athens 07.09.99 Earthquake: The Case of Adámes

The motivation of the present study is to interpret the large concentration of damage to residential and industrial buildings, which occurred in regions near the banks of the Kifisos river canyon during the 7 September 1999 M_s 5.9 Athens Earthquake. In particular, one such region that experienced unexpectedly heavy damage was the small community of Adámes, which borders the canyon at its deepest point, and in which damage was concentrated within 50 m from the crest of the cliff.

Some of the seismological and structural aspects of the earthquake are pictorially summarised in Fig. 3. Notice in particular that the region of Adámes is the most distant region that experienced Modified Mercalli Intensity (MMI) of IX^-. Several other towns and communities, despite being closer to the seismogenic fault, experienced lighter and much lighter damage with MMI values of VIII and VII, respectively. Certainly, soil amplification effects played a substantial role in this non-uniform geographic distribution of damage [Gazetas, 2001].

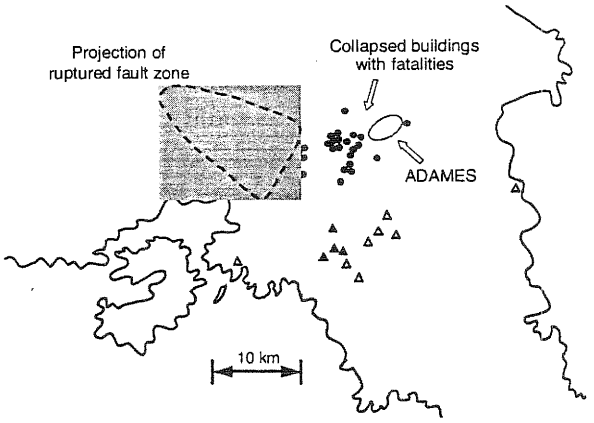

(a)

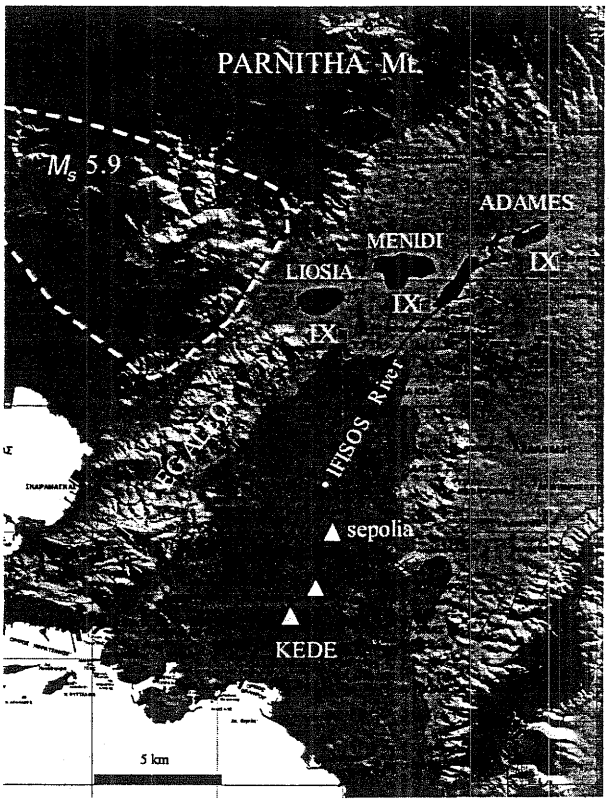

(b)

Fig. 3. (a) Geography of the Athens (Parnitha) Earthquake: projection of seismic source, location of collapsed buildings with fatalities, and location of seismograph stations. (b) 3D view of the Athens Metropolitan area showing the areas that experienced the highest Modified Mercalli Intensity IX$^-$: Adámes, Menidi and Liosia. (c) Distribution of heavy damage in Adámes, showing largest concentration in Site 3, near the crest of Kifisos canyon.

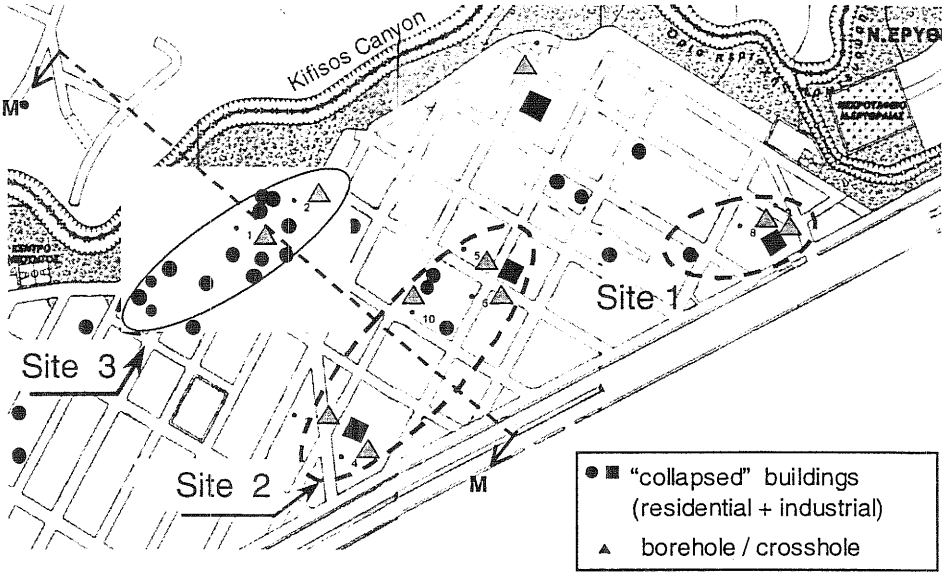

(c)

Fig. 3. (*Continued*)

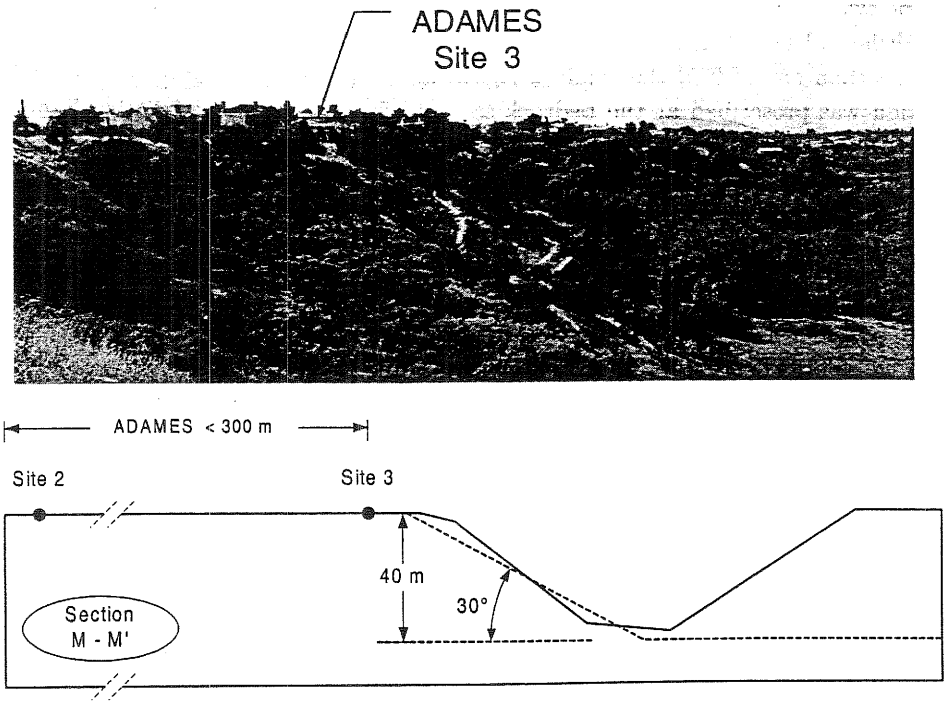

Fig. 4. Typical cross section of the topographic relief of Kifisos river canyon and the region of Adámes. The idealised geometry used in the foreseeing 2D analyses is also shown (dashed line).

Furthermore, even within the small-size community of Adámes, the distribution of damage was hardly uniform. The heaviest concentration of collapsed buildings occurred within one block from the crest of the deepest part of the Kifisos canyon (depth of 40 m). The work presented herein was prompted by the need to explain the causes of such a concentration.

In an earlier paper [Gazetas, 2001], an analysis of the site of interest has been conducted using the actual soil profile and real accelerograms (recorded during the particular earthquake) as input motions. In the present paper, the geometry configuration shown in Fig. 4 is analysed, using initially a simple soil structure to reveal the significance of layering. Other potentially detrimental effects and wave propagation issues are explored in detail for the soil site-specific conditions, namely: (i) the role of the "parasitic" collateral acceleration (either vertical or horizontal) arising from the topographic irregularities, (ii) the presence of a simultaneous vertical P-wave excitation component in addition to the vertical SV excitation, and (iii) the effect of the obliquity of the incident wave motion.

4. Two-Dimensional Modelling of the Problem

The two-dimensional wave propagation analyses were performed with the finite-element code ABAQUS [Hibbit *et al.*, 1997] and the spectral-element code AHNSE [Casadei and Gabellini, 1997; Faccioli *et al.*, 1997]. The finite-element discretisation of the two-dimensional model is shown in Fig. 5(a). The mesh consists of 4-noded quadrilateral and 3-noded triangular elements, the size of which was selected to be less than one-fifth of the smallest significant considered wavelength. The input motion was prescribed at the bedrock-soil interface through transmitting boundaries whilst the vertical lateral boundaries have been placed far enough from the topographical irregularity, where free-field motion could be assumed. The spectral element discretisation for the code AHNSE (Fig. 5(b)) consists of macro-elements, each subdivided into 16 microelements, again with the element size being tailored

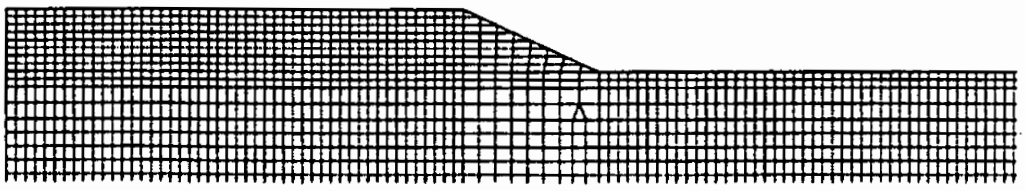

Fig. 5(a). Finite element discretisation of the analysed configuration for the code ABAQUS.

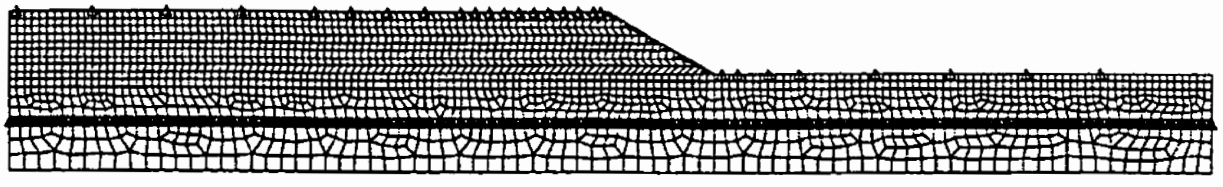

Fig. 5(b). Spectral element discretisation of the analysed configuration for the code AHNSE.

to the propagating wavelengths. In this case, absorbing boundaries were placed around the domain of interest.

Another difference between the two codes relates to the way material damping is introduced in the analysis. In ABAQUS, material damping is of Rayleigh type and therefore frequency dependent. In the present study, the required damping ratio was assigned to the fundamental frequency of the soil stratum and the central frequency of the input motion, and successively the coefficients of Rayleigh damping were computed. In AHNSE, material damping is of viscous type, which means that damping is frequency independent. A complete description of how the hysteretic nature of damping is simulated with a viscous model can be found in the general description of the computer code. In the context of the present study it was found that the best convergence was achieved when the viscosity coefficient was calculated using the mean frequency of the velocity spectrum of the input motion.

Notwithstanding the aforementioned constitutive differences in the analysis algorithms, compatibility of the two approaches (a prerequisite for accepting the results) was achieved easily.

Vertical and inclined plane SV and P waves describe the "rock outcrop" excitation in the foregoing analyses, with the time function for all cases studied being a Ricker wavelet of type Beta:

$$u(t) = [1 - 2b(t - t_0)^2] \exp[-b(t - t_0)^2],$$

where $b = (\pi f_0)^2$, with f_0 as the characteristic frequency, and t_0 is time of $\max[u(t)]$.

5. Parametric Study: Effect of Soil Stratigraphy on 2D Wave Amplification

To investigate the significance of soil layering, the fundamental case of a homogeneous layer with the geometry of Fig. 5 subjected to a Ricker type excitation with $f_0 = 3$ Hz is first analysed. We chose shear wave velocity $V_s = 500$ m/s (typical value for the stiff clays and marls encountered in the earthquake-stricken region) and material damping $\xi = 5\%$.

Then, the configuration sketched in Fig. 6 is analysed. The effect of the relative thickness and impedance ratio of the surface layer with respect to the underlying soil

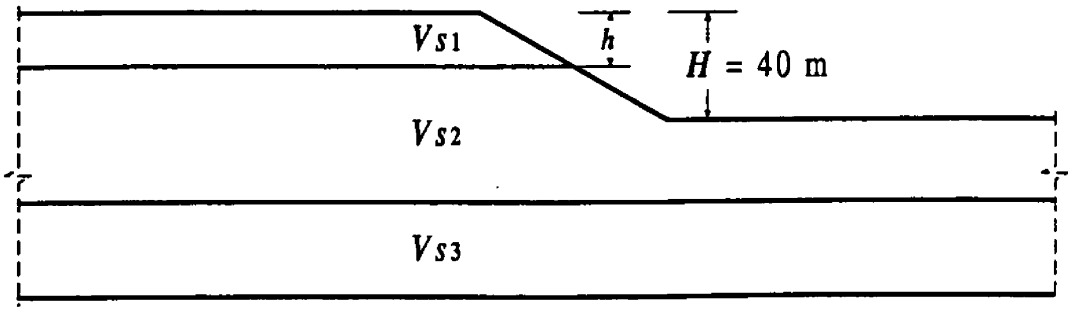

Fig. 6. Geometrical configuration and layered structure of the profile used in the foregoing studies.

Table 1. Layer thickness and soil properties of the parameters study.

	Case		h/H	V_{S1}/V_{S2}	V_{S2}/V_{S3}	V_{S3} [m/s]
Homogeneous halfspace	1		–	1	1	500
Surface stiff layer	2	a	0.25	2	0.75	750
		b	0.5	2	0.75	750
Surface soft layer	3	a	0.25	0.5	0.75	750
		b	0.5	0.5	0.75	750
Homogeneous layer over bedrock	4	a	–	1	0.75	750
		b	–	1	0.5	1000
		c	–	1	0.2	5000

deposit, as well as the effect of the soil-bedrock impedance ratio are parametrically examined. The studied cases are outlined in Table 1. Material damping of the soil layers is maintained at the level of 5% (which actually corresponds to the average value of the one-dimensional equivalent linear analyses performed for the actual soil profile of the analysed site).

The analysed cases are compared in terms of: (i) the computed horizontal acceleration time histories at distances $x = 10$ m and $x = 300$ m from the cliff, (ii) the normalised peak acceleration with respect to the free-field motion (defined at $x = 300$ m from the river cliff), (iii) the spectrum of the Topographic Aggravation Factor (TAF), defined as the ratio of the Fourier amplitude spectrum of the motion at $x = 10$ m to the free-field motion ($x = 300$ m), and (iv) the ratio of the parasitic vertical motion, the result of wave diffraction. Finally, we also examine the transfer functions between the free-field motion at the outcropping of layer 2 (on the right side of the cliff) and the positions at $x = 10$ m and $x = 300$ m from the cliff. These functions encompass not only the effect of the presence of the topographic irregularity on the surface response of the model, but also the effect of 1D *soil flexibility* on the absolute amplification (or de-amplification) of the input motion.

It is noted that the distance from the edge of the cliff beyond which the influence of the topographic irregularity is negligible (i.e. the distance to the free-field) is a function of the frequency of the excitation for a given geometry. For the studied cases, the distance $x = 300$ m was found to invariably belong to the free field.

In Figs. 7(a) and 7(b) the acceleration time histories computed at the surface of the analysed model are shown, at distances $x = 10$ m and $x = 300$ m from the cliff, for the surface *stiff* ($V_{S1}/V_{S2} = 2$) and *soft* ($V_{S1}/V_{S2} = 0.5$) layer cases respectively. As it can be readily seen, two-dimensional amplification is present in all cases, as the edge amplitude is invariably higher than that of the free-field. Yet, soil layering and flexibility also plays a decisive role in the response. Specifically, in the cases of the homogeneous halfspace (Case 1) and of the stiff surface layer (Cases 2) the soil de-amplifies the motion, while it amplifies the motion in Case 3. Please notice that the above de-amplification is due solely to the fact that the dominant

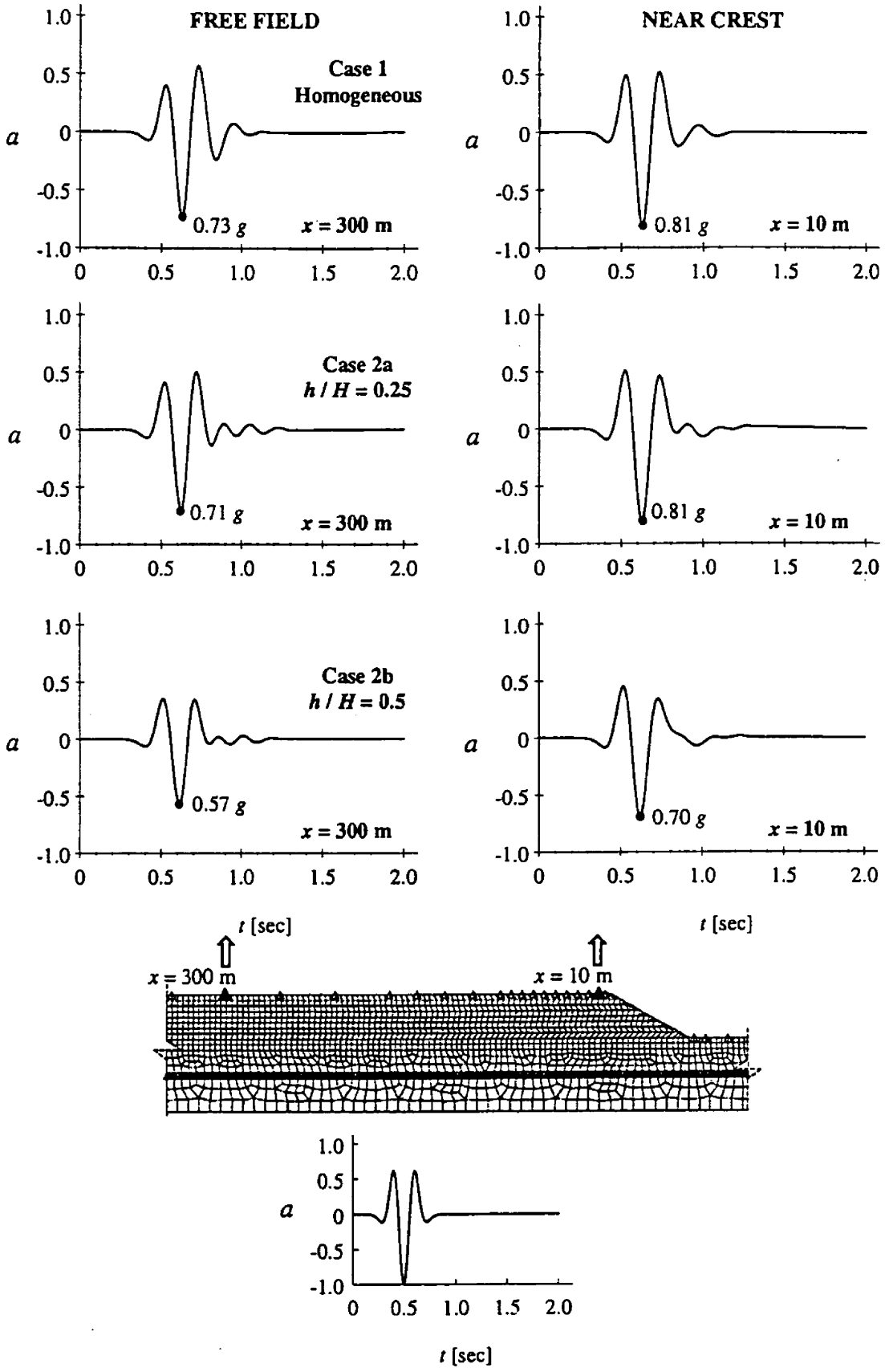

Fig. 7(a). Computed time histories of horizontal acceleration at $x = 10$ m and $x = 300$ m, for Case 1 (homogeneous) and Cases 2a and 2b (*stiff surface layer*: $V_{S1}/V_{S2} = 2$). Rock outcrop excitation: vertical SV, Ricker $f_0 = 3$ Hz, PGA = 1.

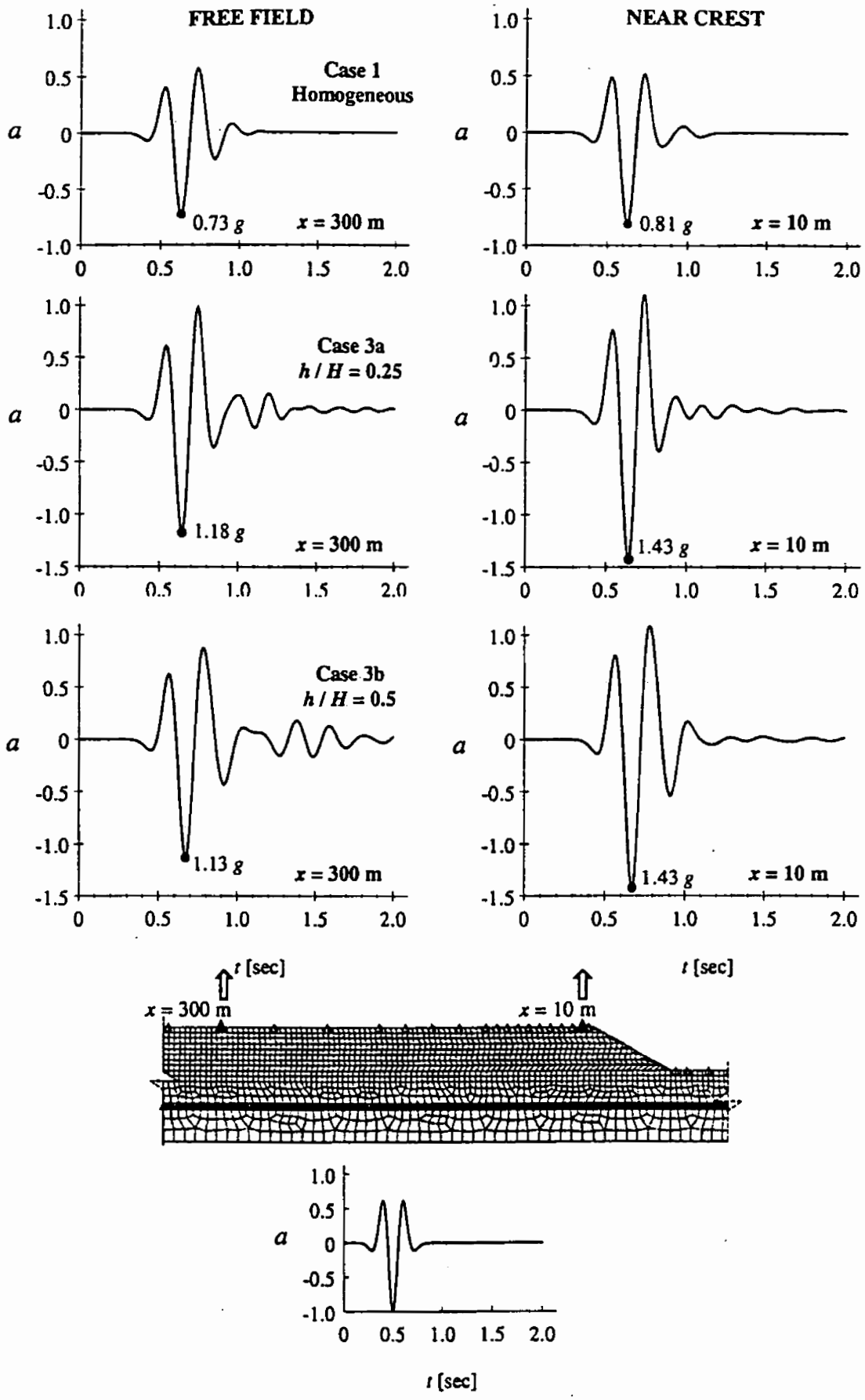

Fig. 7(b). Computed time histories of horizontal acceleration at $x = 10$ m and $x = 300$ m, for Case 1 (homogeneous) and Cases 3a and 3b (*soft surface layer*: $V_{S1}/V_{S2} = 0.5$). Rock outcrop excitation: vertical SV, Ricker $f_0 = 3$ Hz, PGA = 1.

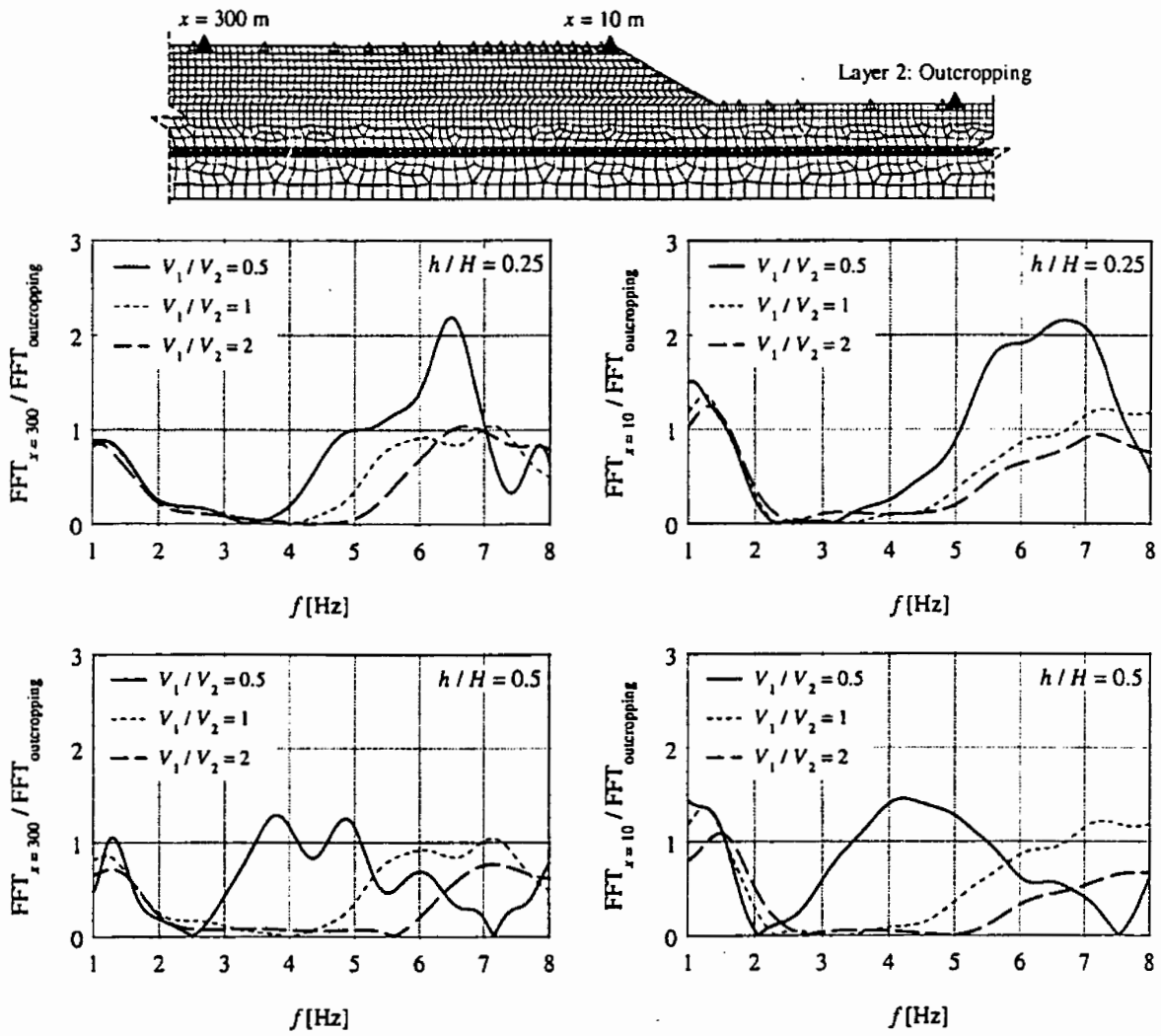

Fig. 8. Effect of the relative stiffness and thickness of the top layer, on the transfer function between the outcropping of layer 2 and positions: (a) $x = 10$ m from the crest on the right, and (b) $x = 300$ m from the crest on the left.

frequencies of the Ricker excitation exceed appreciably the fundamental frequency of the bank profile. This is a coincidence which should not be unduly generalised. The fact remains that even in this case the 2D effect is detrimental. This becomes also apparent in Fig. 8, where the effect of the presence of the surface layer is explored in terms of the transfer functions of the motion from the outcropping of layer 2 to distances $x = 10$ m and $x = 300$ m from the crest.

Figure 9 portrays the distribution along the ground surface of the normalised peak horizontal acceleration (with respect to the free-field maximum amplitude), for the homogeneous, soft layer and stiff layer cases. As it can be readily seen, for the homogeneous case, the topography effect is noticeable, yet not as substantial as for the layered medium. In addition, for the *soft surface layer* case, the thickness of the surface layer has little impact on the distribution of the normalised acceleration — in contrast to the *stiff surface layer* case, in which the zone of influence of the cliff increases with the thickness of the surface layer.

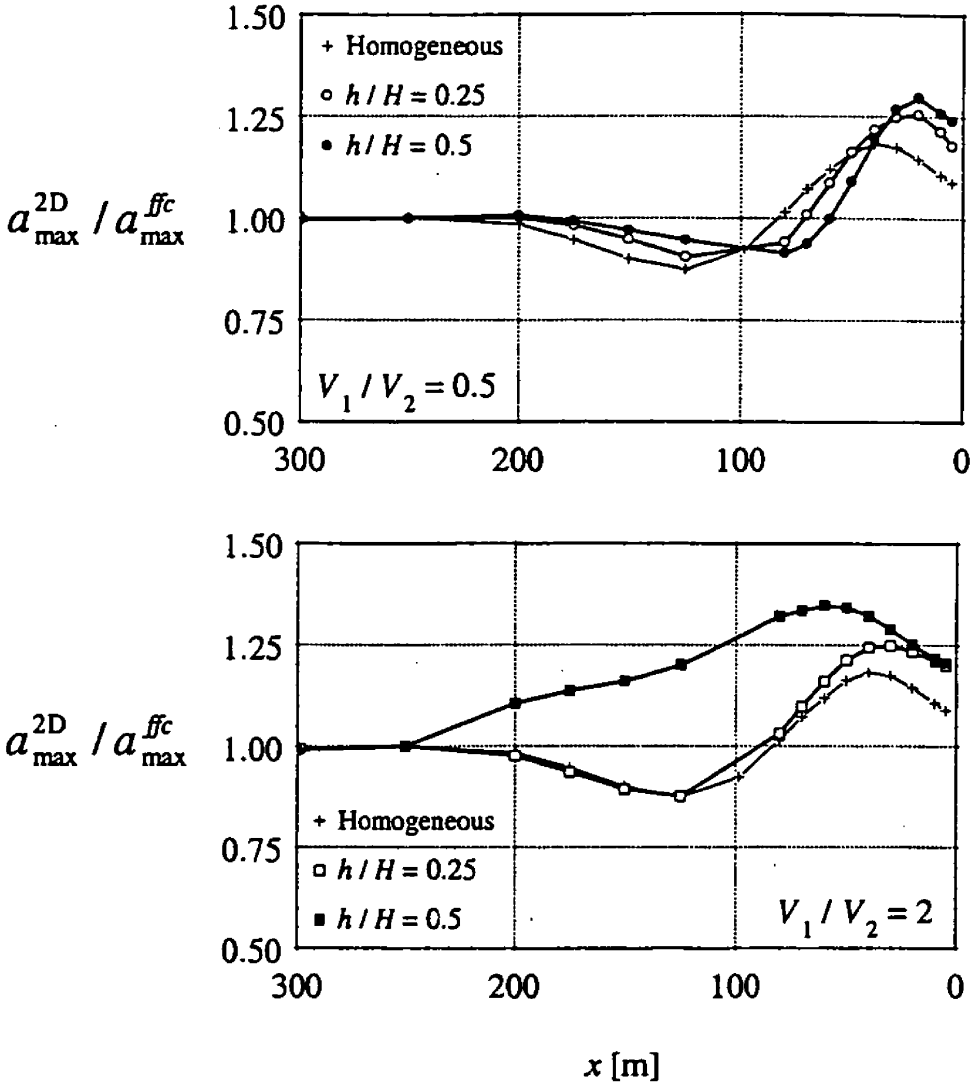

Fig. 9. Effect of relative stiffness and thickness of the surface layer, on the normalised peak acceleration, for the (top) and *stiff* (bottom) *surface soft* layer model, with a Ricker ($f_0 = 3$ Hz) wavelet as vertical SV wave excitation.

A more useful measure of topographic amplification in the frequency domain is defined as the ratio of the Fourier amplitude spectra at $x = 10$ m (close to the crest) and at $x = 300$ m (defined as the *free-field* motion). Named ***Topographic Aggravation Factor***, this ratio (denoted as TAF) is plotted in Fig. 10 as a function of frequency, f, for the *homogeneous*, *soft layer* and *stiff layer* cases.

As it can be readily seen, topographic amplification of the motion is certainly more pronounced for a layered medium (at least in the frequency range 3–6 Hz) — since multiple reflections and/or transmissions of the vertical incident S-waves on/through the horizontal layer interfaces lead to additional amplification of the motion near the crest (apart from the diffracted waves, which are also present in the homogeneous case). Moreover, topographic amplification is more apparent in the soft surface layer case, which in fact was the characteristic of the profile in Site 3 (region located next to the cliff and severely damaged during the 7 September 1999 Athens earthquake). As for the normalised peak acceleration, the thickness of the

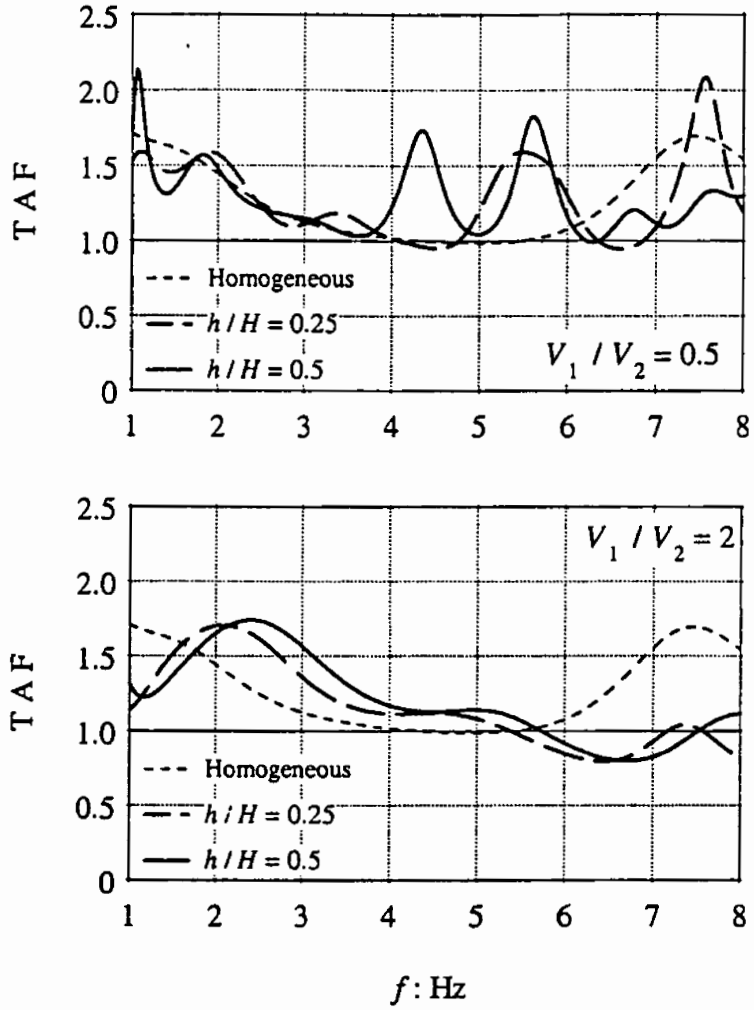

Fig. 10. Effect of the relative stiffness and thickness of the surface layer, on the spectrum of the Topographic Aggravation Factor (TAF), for the *soft* (top) and *stiff* (bottom) *surface* soil layer model, with a Ricker ($f_0 = 3$ Hz) wavelet as vertical SV wave excitation.

surface layer does not significantly affect the level of the computed TAF, both for the soft layer and stiff layer cases.

It should be noted herein that for both the soft layer and the stiff layer cases, the first peak in the TAF spectrum corresponds approximately to the fundamental frequency of the one-dimensional soil column behind the crest (i.e. the profile in the free-field). Nevertheless, since the effect is obviously frequency-dependent, the broadband nature of the Ricker wavelet used in the present study might not emphasise the potential importance of certain frequencies (for the soil properties used in the present simulations).

The effect of the relative stiffness and thickness of the surface layer is illustrated in Fig. 11 in terms of the distribution of the normalised *parasitic* vertical acceleration along the ground surface. This is denoted so, to emphasise the fact that there is an accompanying vertical component which develops collaterally — arising not only from direct P and inclined SV waves, but also from waves diffracted due to the presence of the topographic irregularity.

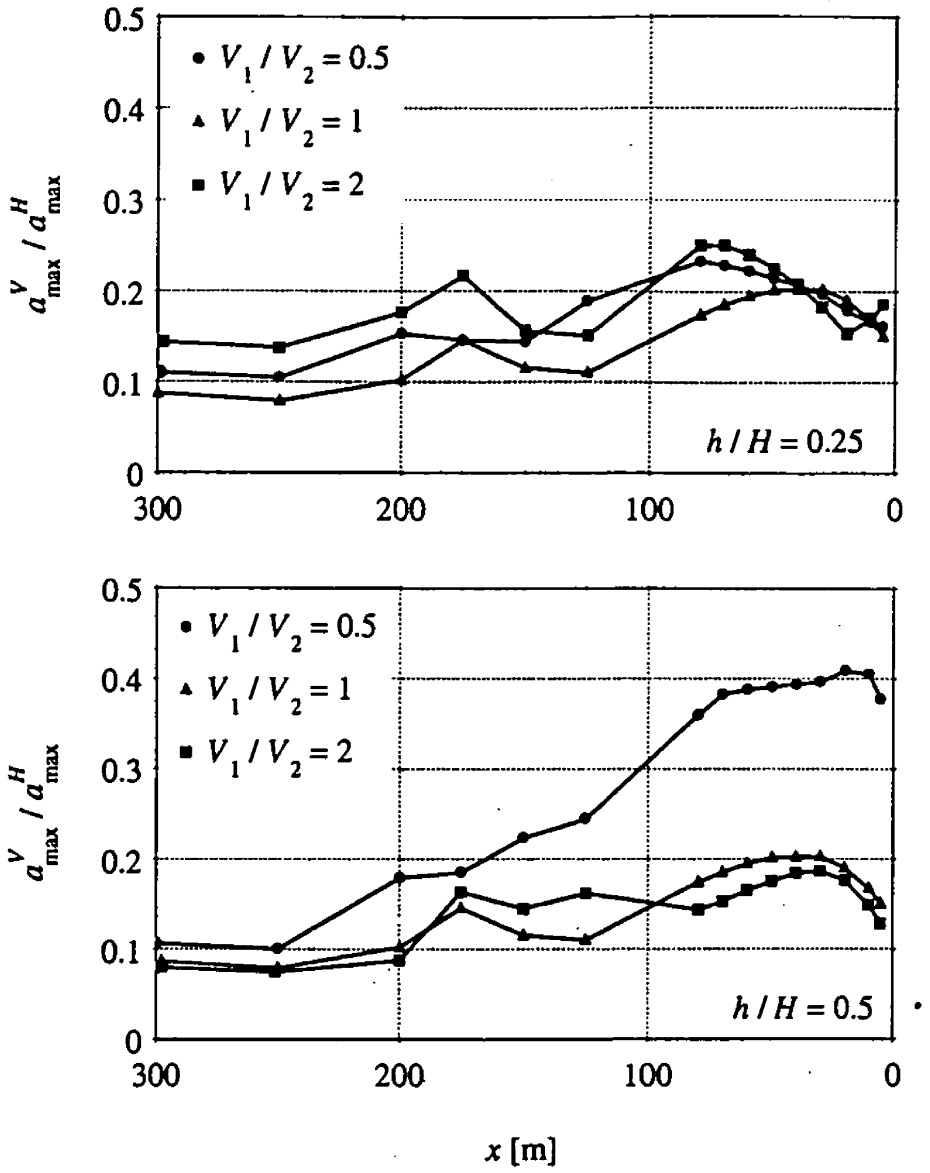

Fig. 11. Effect of relative stiffness and thickness of the surface layer, on the distribution of the normalised peak vertical acceleration. Excitation: vertical SV wave Ricker ($f_0 = 3$ Hz) wavelet.

For Cases 2a and 3a ($h/H = 0.25$), it is observed that the vertical component may obtain values as high as $a_V \approx 0.25\ a_H$, and its amplitude and spatial distribution pattern are practically invariant with the stiffness of the surface layer. However, for Case 2b ($h/H = 0.5$, $V_{s1}/V_{s2} = 0.5$), the peak acceleration of the "parasitic" component becomes almost $a_V \approx 0.40\ a_H$ — approximately of the order of magnitude estimated for the actual soil profile in Adámes.

Finally, the effect of the impedance of the bedrock (layer 3) to the overlying soil deposit (Cases 4a–4c with $V_{s1}/V_{s2} = 1$) is also explored. For this purpose, the distribution of the normalised peak horizontal and vertical acceleration along the ground surface, and the spectrum of the Topographic Aggravation Factor are evaluated. Results are summarised in Fig. 12, where it becomes apparent that increasing the bedrock stiffness, topographic effects are aggravated, since the energy of the incoming motion is simultaneously one-dimensionally and two-dimensionally

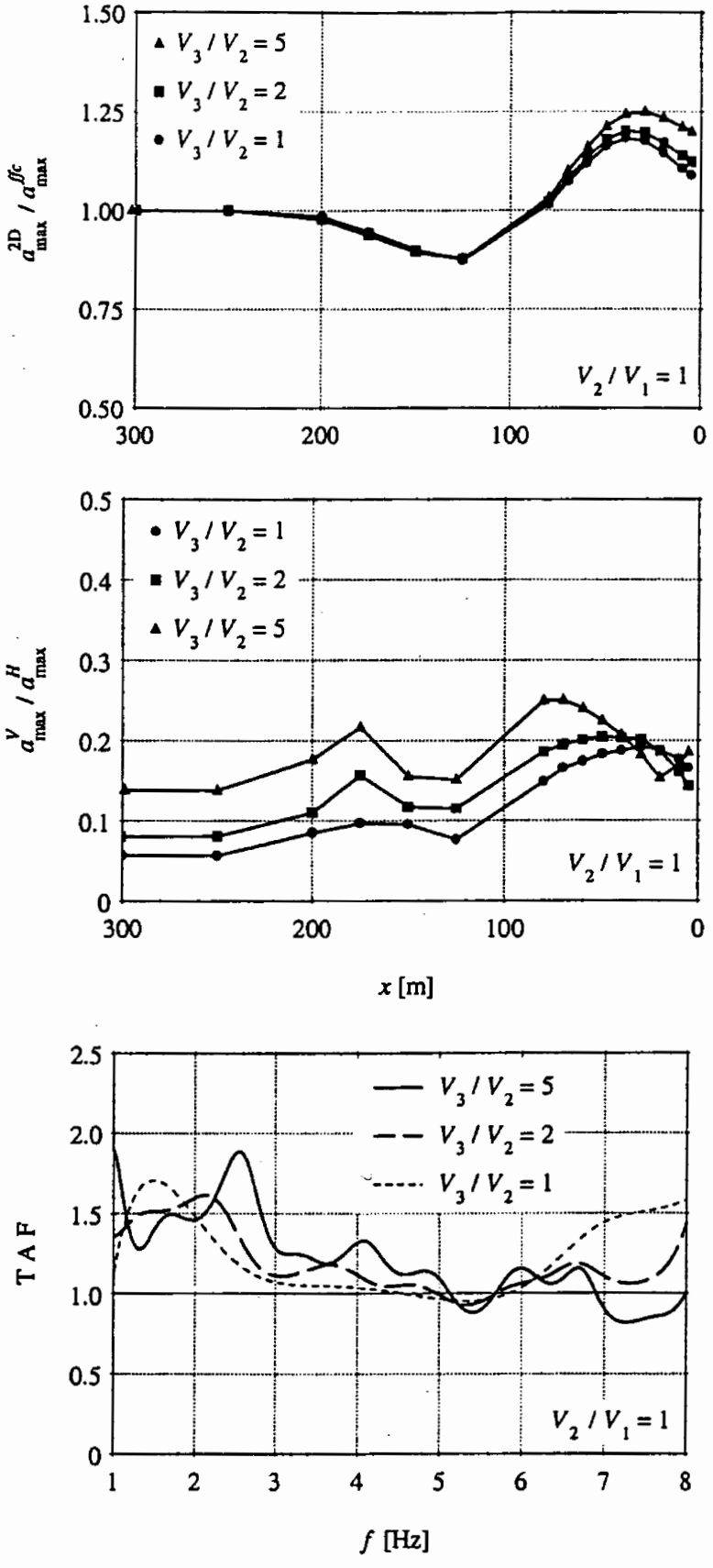

Fig. 12. Effect of the ratio of impedances of the bedrock to the overlying soil deposit, on the distribution of the normalised horizontal and vertical peak acceleration, and the spectrum of the Topographic Aggravation Factor. Excitation: vertical SV wave Ricker ($f_0 = 3$ Hz) wavelet.

amplified within the soil layer. For the peak horizontal acceleration, this effect is restricted to a zone approximately 50 m from the crest, whereas the impact on the normalised peak vertical acceleration is apparent even in the free field.

In the view of the results shown above, it is concluded that the soil stratigraphy plays a very significant role in modulating the surface response, resulting either in amplification or even in de-amplification of the input motion under certain site conditions. The relative stiffness of the surface layer has been proven to be the most important parameter. For the soft layer case, the incident wave is trapped within the surface layer undergoing multiple reflections (one-dimensional amplification), and further amplified from diffractions due to the two-dimensional nature of the problem. For the stiff layer case, most of the incoming energy is reflected towards the halfspace (one-dimensional de-amplification), at the interface of the surface with the underlying soil layer, and diffractions at the topographic irregularity are not sufficient to amplify the absolute incoming motion.

It should be noted herein that the thickness of the surface layer, once being of the same order of magnitude with the incident wavelengths, is not a decisive parameter, affecting however: (i) the spatial distribution of the normalised acceleration in the hard layer case, where the incoming motion is de-amplified in terms of absolute acceleration levels, (ii) the frequencies of the input motion to be amplified or de-amplified, in accordance to the resonant frequencies of the one-dimensional soil column behind the crest, and (iii) the magnitude and spatial distribution of the "parasitic" vertical component, which may be as significant as 40% of the peak horizontal acceleration.

Finally, the relative stiffness of the underlying bedrock is proven to be less important in the evaluation of the response. In Cases 4a–4c examined herein, the overlying soil deposit is homogeneous and therefore incoming waves do not undergo multiple reflections/transmissions at the layer interfaces which would result in further amplification of the surface response.

6. Site Specific Analyses

In the ensuing, the effects of the frequency content of the input motion and the type and direction of the incident wavefield will be examined in conjunction with the stratigraphy of three characteristic soil profiles in the region of Adámes. The Profiles A–C used in the analysis, have been constructed according to the geotechnical investigation conducted on site, comprising both of in-situ and laboratory tests.

Two-dimensional analyses are performed for the geometry configuration shown in Fig. 7, and horizontal layering is assumed for all three profiles under consideration. To account for the nonlinear soil behaviour under seismic wave propagation, the analysis consists of two parts: (i) equivalent linear one-dimensional analyses for the soil Profiles A–C, and (ii) two-dimensional elastic analyses using the soil properties evaluated at the last step of the iterative algorithm (reduced stiffness and

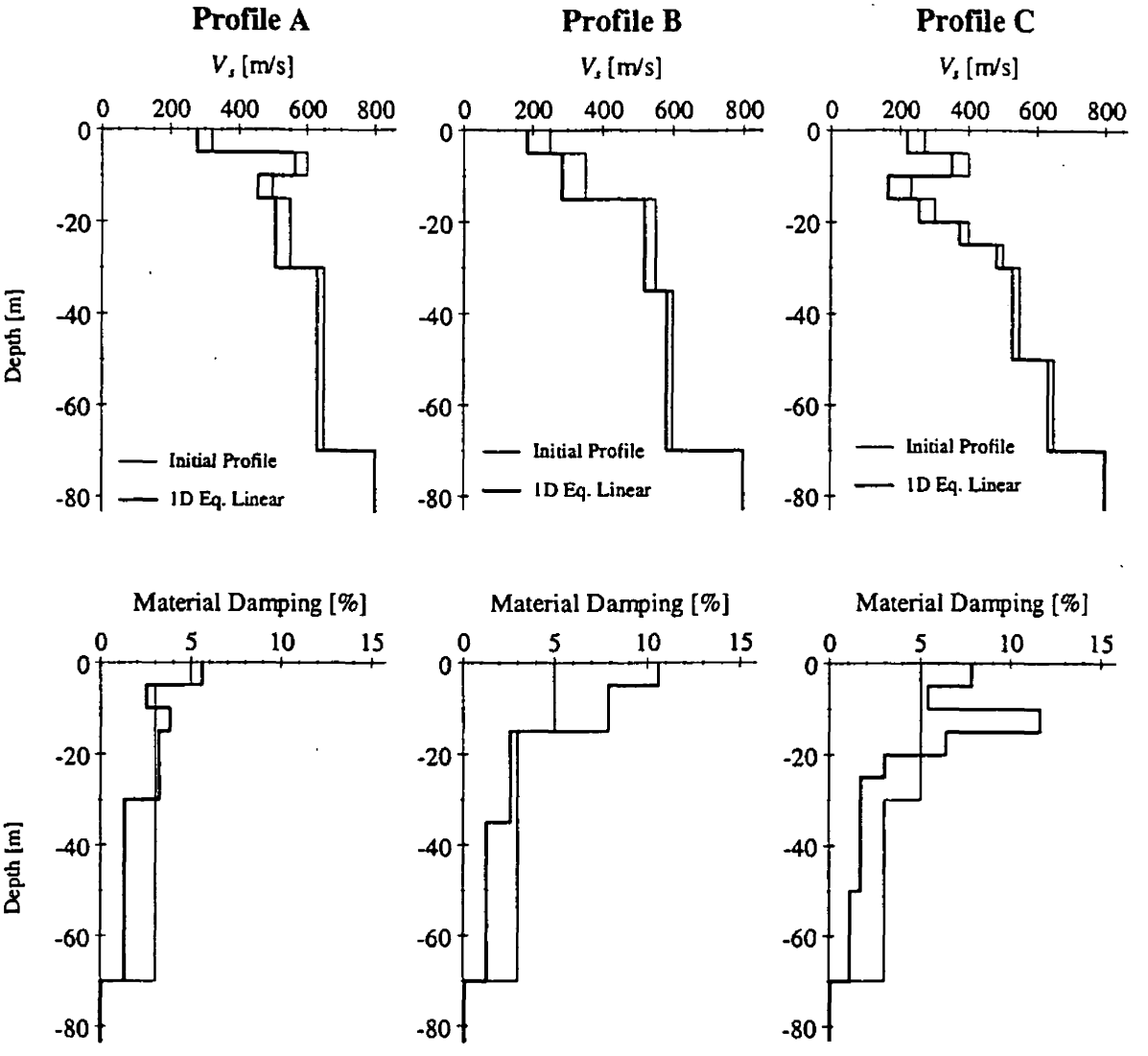

Fig. 13. Three shear wave velocity (V_s) and hysteretic damping ratio profiles: The zero-strain (elastic) velocities, based on cross-hole measurements in Adámes, and the initial estimates of damping are shown in "fade" line. The strain-compatible values of V_s and damping, obtained from 1D wave response analyses are shown in bold line.

material damping, adjusted to the levels of strain exhibited by the one-dimensional soil column).

These three soil profiles are shown in Fig. 13, whilst detailed description of the aforementioned analysis can be found in Gazetas *et al.* [2002]. The fundamental frequencies of the three profiles — based on the reduced soil parameters evaluated at the last iteration of the equivalent linear analysis — are: (i) $f_1 = 2.15$ Hz for Profile A, (ii) $f_1 = 1.72$ Hz for Profile B, and (iii) $f_1 = 1.37$ Hz for Profile C.

6.1. *Frequency content of the input motion*

In the present section, the analysed configuration — with a layered soil structure corresponding to the three Profiles described above — is subjected to two different vertical SV Ricker wavelets, with central frequencies $f_0 = 3$ Hz and $f_0 = 5$ Hz.

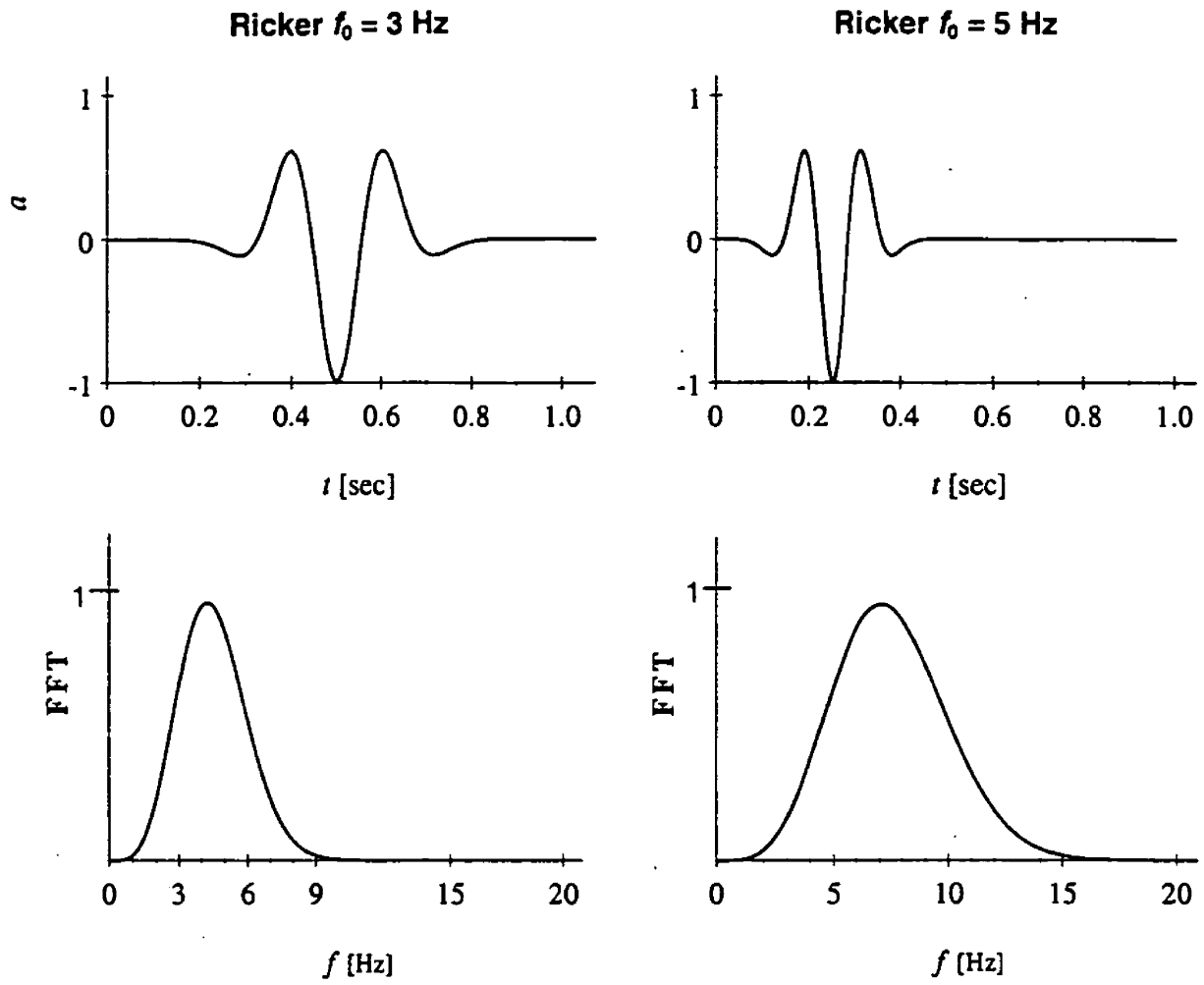

Fig. 14. Normalised time histories and corresponding Fourier amplitude spectra of Ricker $f_0 = 3$ Hz (left) and $f_0 = 5$ Hz (right) wavelets.

The time histories and Fourier spectra of the two wavelets used are illustrated in Fig. 14. The scope of the following analysis is to investigate: (i) the effect of the frequency content of the excitation on the distribution of the normalised maximum horizontal (a_H) and vertical acceleration (a_V) along the ground surface behind the crest, and (ii) the sensitivity of the Topographic Aggravation Spectrum (TAF) to the frequency content of the selected input motion.

In what follows, Fig. 15 portrays the distribution of the normalised peak horizontal acceleration a_H (with respect to the free-field motion) for the two input motions under investigation, and Fig. 16, the distribution of the normalised peak vertical acceleration a_V (with respect to maximum horizontal acceleration at the same location). Finally, the stability of the computed TAF (for the specific geometry and soil profile) with respect to the frequency content of the input motion is investigated in Fig. 17.

As it can be readily seen in Fig. 15, the frequency content of the excitation (Ricker wavelet) significantly affects the magnitude and distribution of the normalised peak horizontal acceleration (a_H) along the ground surface behind the

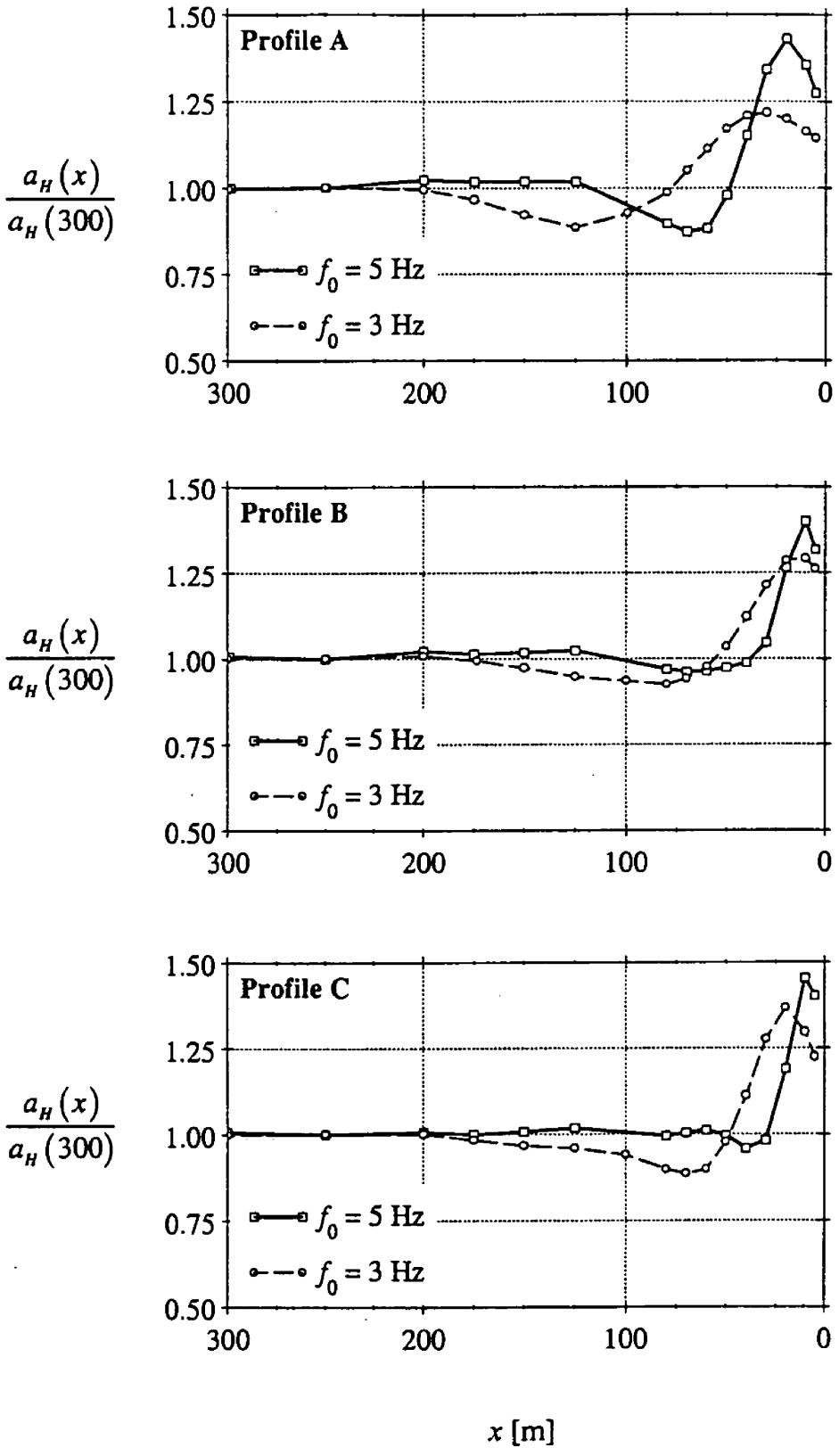

Fig. 15. Effect of the frequency content of the input motion and the exact soil profile, on the normalised peak horizontal acceleration, with Ricker $f_0 = 3$ Hz and $f_0 = 5$ Hz wavelets as vertical SV wave excitation.

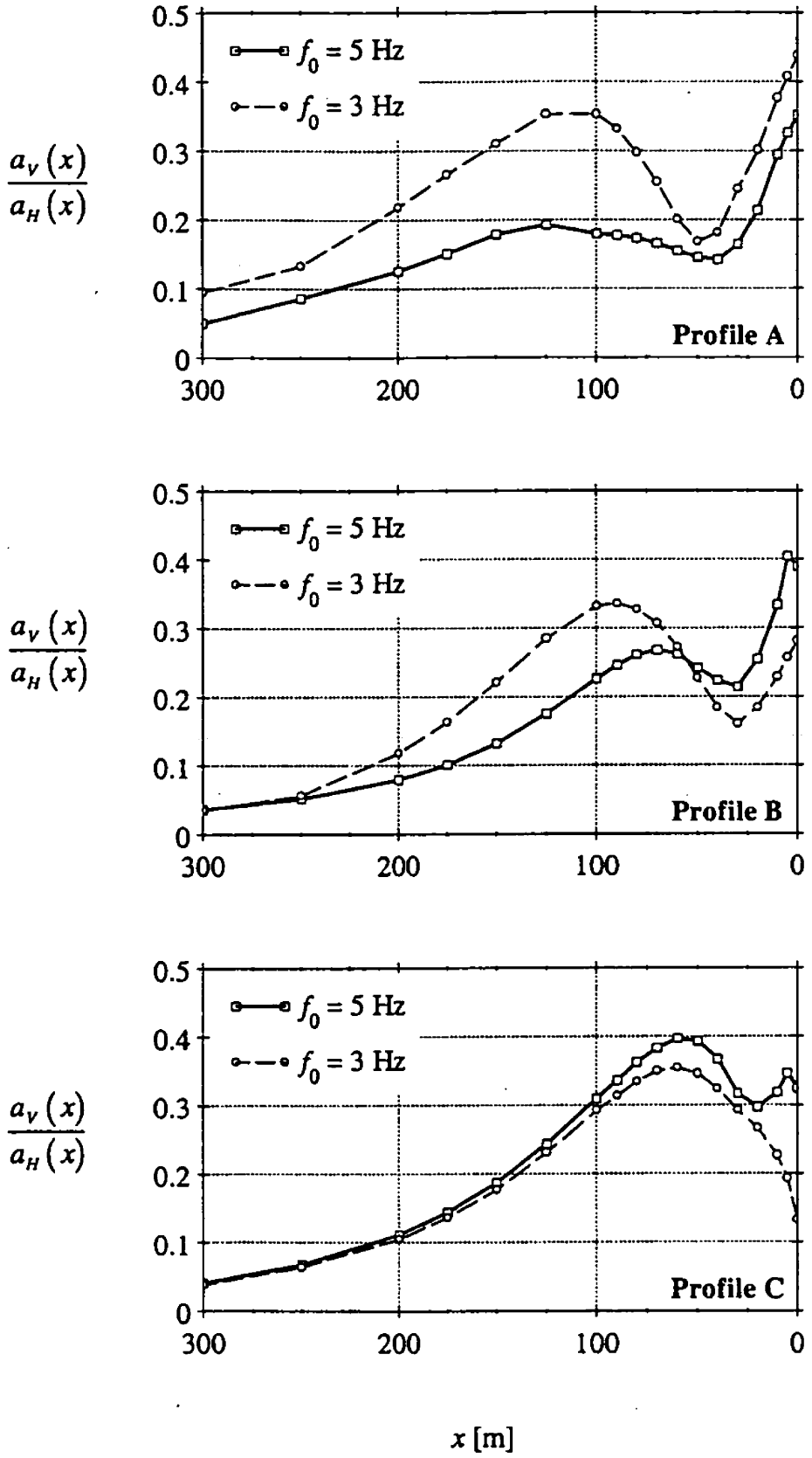

Fig. 16. Effect of the frequency content of the input motion, on the relative magnitude of the peak vertical acceleration which "parasitically" develops as a result of 2D wave scattering even with a purely horizontal excitation, consisting of vertically incident SV Ricker waves with $f_0 = 3$ Hz and $f_0 = 5$ Hz.

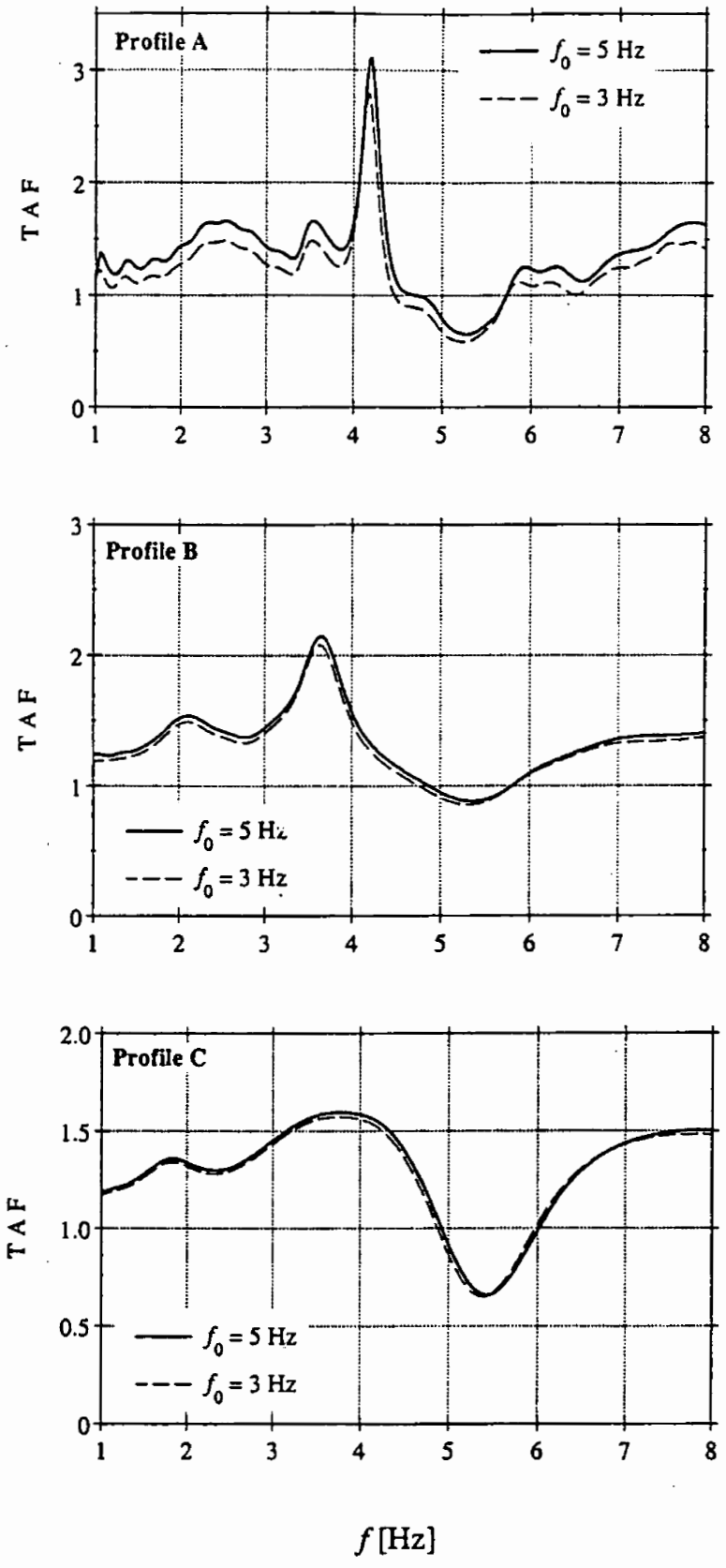

Fig. 17. Effect of the frequency content of the input motion, on the spectrum of the Topographic Aggravation Factor (TAF), with Ricker $f_0 = 3$ Hz and $f_0 = 5$ Hz wavelets as vertical SV wave excitation. As expected, being the ratio of two output Fourier spectra, TAF is independent of the frequency (and amplitude) of the input motion.

slope crest. In particular, increasing the central frequency of the Ricker wavelet results in increasing the *intensity* of the topography effects, and the phenomenon becomes more apparent as the stiffness of the analysed profile increases. Therefore, for Profile A, the maximum increase of the normalised peak horizontal acceleration is approximately 20%, whereas for the softer Profiles B and C, it is 10% and 8% respectively.

Moreover, the zone of influence of the topographic irregularity decreases as the incident motion becomes richer in high frequencies. Taking under consideration that for a given soil profile, higher frequencies correspond to shorter propagating wavelengths, results are found to be in agreement with similar researches conducted in the past.

Figure 16 shows that the distribution of the normalised peak vertical acceleration (a_V) is also affected by the frequency content of the incident wavelet. In particular, comparing the response of the three profiles under investigation, the normalised amplitude of the *parasitic* acceleration due to the high frequency pulse increases as the stiffness of the layered medium decreases. Nevertheless, the spatial distribution pattern is similar for the two wavelets studied, and the location away from the slope crest, where after the magnitude of the horizontal component is negligible, remains practically invariant.

Finally, investigating the sensitivity of the Topographic Aggravation Factor (TAF) to the selected excitation (Fig. 17), it becomes clear that the TAF spectrum remains practically constant for the range of frequencies of interest (1–8 Hz), regardless of the frequency content of the Ricker wavelet. It should be noted however that for Profile A, which is the stiffer of the three profiles under investigation, the values of the resulting TAF computed for the $f_0 = 5$ Hz Ricker wavelet are approximately 10% higher. This could be attributed to the fact that the high-frequency motion may well have excited resonant frequencies of the specific profile — whilst the effect for the other two profiles is negligible for the frequency range of interest.

It should be pointed out herein that a more rigorous approach of the problem should have included a separate series of equivalent linear one-dimensional analyses for the two input motions under investigation, which would be successively assigned to the two-dimensional model. However, rough preliminary computations performed showed no significant differences for the two approaches.

6.2. *Type of incident waves*

Heretofore, parametric studies have been conducted using solely vertically incident SV waves as input motion. Nevertheless, wave diffraction at the location of the topographic irregularity, produces both Rayleigh and SP waves which propagate along the free surface. Interference between the direct, diffracted, and transmitted and/or reflected at the soil layer boundaries waves, produces a complicated wave pattern which involves — among other — the collateral development of a *parasitic* vertical acceleration component at the ground surface close to the cliff. It should

be also noted that the amplitude of this component has been found to be anything but negligible, reaching in some cases values as high as $a_V = 0.40\ a_H$.

In what follows, a series of analyses are performed, using simultaneously a vertically propagating SV wavelet of Ricker type with central frequency $f_0 = 3$ Hz, and a P-wave with half the amplitude of the SV wave, comprising of a sequence of two Ricker wavelets, with central frequencies: (i) $f_0 = 5$ Hz and $f_0 = 8$ Hz, and (ii) $f_0 = 10$ Hz and $f_0 = 15$ Hz. The incident P-wave has been deliberately selected to contain higher frequencies and to have lower amplitude than the SV wave, attempting to simulate reality. The acceleration time histories used in the analyses are shown in Fig. 18.

It should be noted that indeed, the wave-field pattern for incident P-waves is simpler than for incident SV waves, partly due to the absence of diffracted SP waves (in this case, diffraction produces primarily Rayleigh waves), and partly due to the relatively longer wavelength of P-waves for a given period. According to Bard [1982], incident SV waves possess the greatest scattering power and they seem to be associated with the most complicated diffraction scheme.

In what follows, elastic two-dimensional analyses are conducted for the geometry configuration of Fig. 5, and the Profiles A–C described in Fig. 14. For the case of

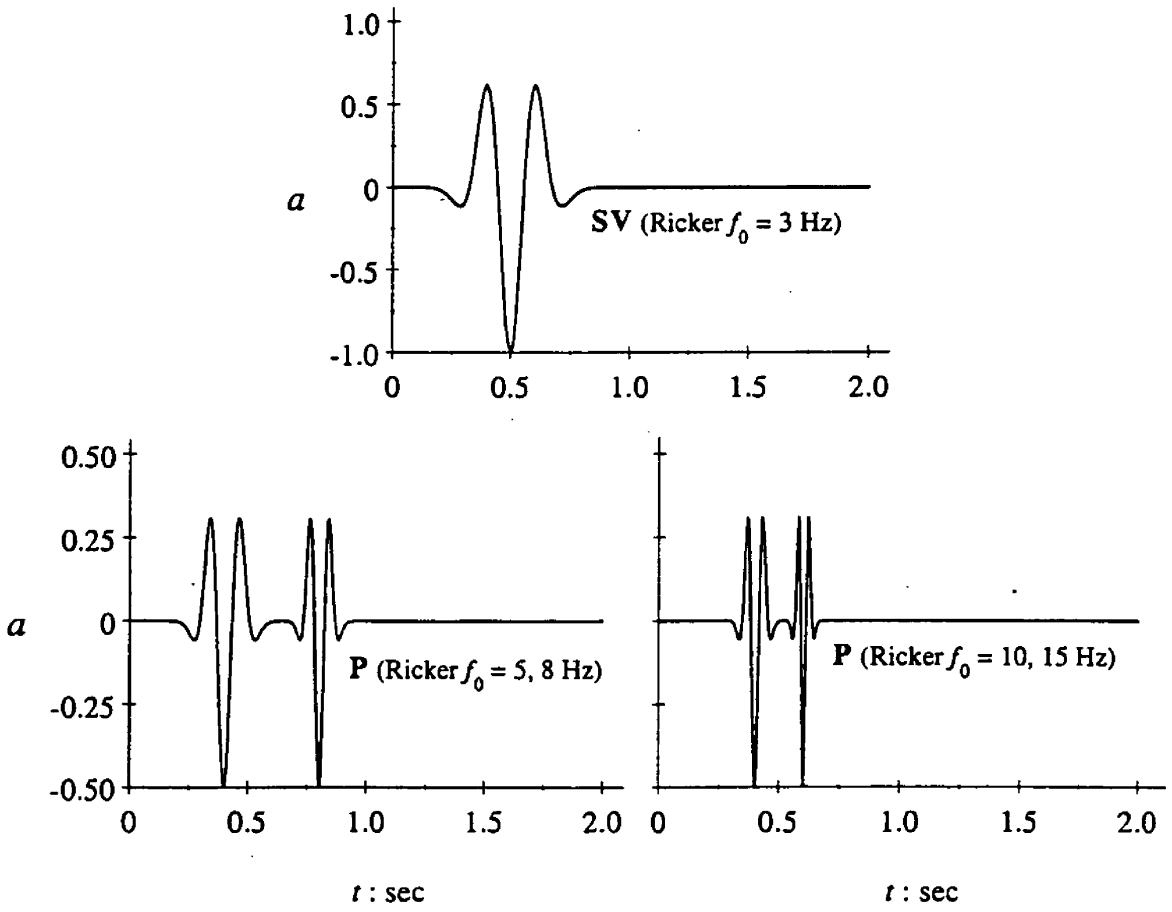

Fig. 18. SV and P wave Ricker type acceleration histories used in the analysis.

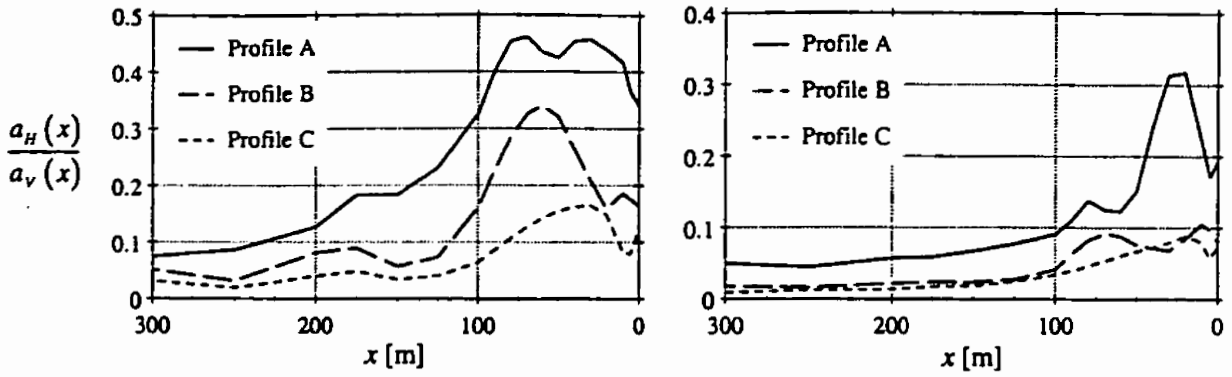

Fig. 19. Distribution of the ratio of horizontal ("parasitic") to vertical acceleration on the ground surface for the three Profiles (A–C) under investigation with Ricker type wavelets $f_0 = 5$ and 8 Hz (left) and $f_0 = 10$ and 15 Hz (right) wavelets as P-wave excitation.

incident P-wave Ricker pulses, the results are portrayed in Fig. 19, in terms of the normalised *parasitic* horizontal acceleration component, for the two excitations under consideration.

Successively, the horizontal acceleration time histories, resulting from the separate analyses of incident SV and P waves, are superimposed at the location $x = 10$ m from the crest, for the three Profiles A–C. The resulting response is shown in Figs. 20(a)–(c). Finally, the effect of the presence of the simultaneous vertical excitation in terms of the Topographic Aggravation Factor spectrum (TAF), computed for the topographic (two-dimensional) amplification of the horizontal acceleration, is also portrayed in Figs. 20(a)–(c).

As it can be readily seen, the presence of a simultaneous vertical excitation significantly affects the response of the stiffer layered structure (Profile A) — a fact that is not surprising since the vertical motion is rich in high frequency components — and the effect is expected to be less apparent as the stiffness of the analysed profile decreases.

In particular, for the P-wave excitation consisting of a sequence of Ricker pulses with $f_0 = 5$ Hz and $f_0 = 8$ Hz, the *parasitic* horizontal component (due to the vertical excitation) is mainly present in a zone approximately 100 m from the crest, and for Profile A takes values which can be as high as 45% of the maximum vertical acceleration at the corresponding location. For the high frequency vertical motion (a sequence of Ricker pulses with $f_0 = 10$ Hz and $f_0 = 15$ Hz), the effect is confined in a narrower zone close to the cliff, yet again for Profile A, the magnitude of the peak *parasitic* horizontal acceleration is approximately $a_H = 0.30\, a_V$.

The effects of the simultaneous incidence of SV and P waves on the absolute magnitude of horizontal acceleration, at distance $x = 10$ m from the cliff, are summarised below. For the P-wave with the $f_0 = 5$ and 8 Hz: (i) the maximum amplitude of the motion is 12% higher for Profile A, when compared to the response to a single SV incident Ricker pulse with central frequency $f_0 = 3$ Hz, and (ii) the effect is less apparent for Profiles B and C. For the P-wave with the $f_0 = 10$ and 15 Hz, the effect is almost negligible for all profiles under consideration.

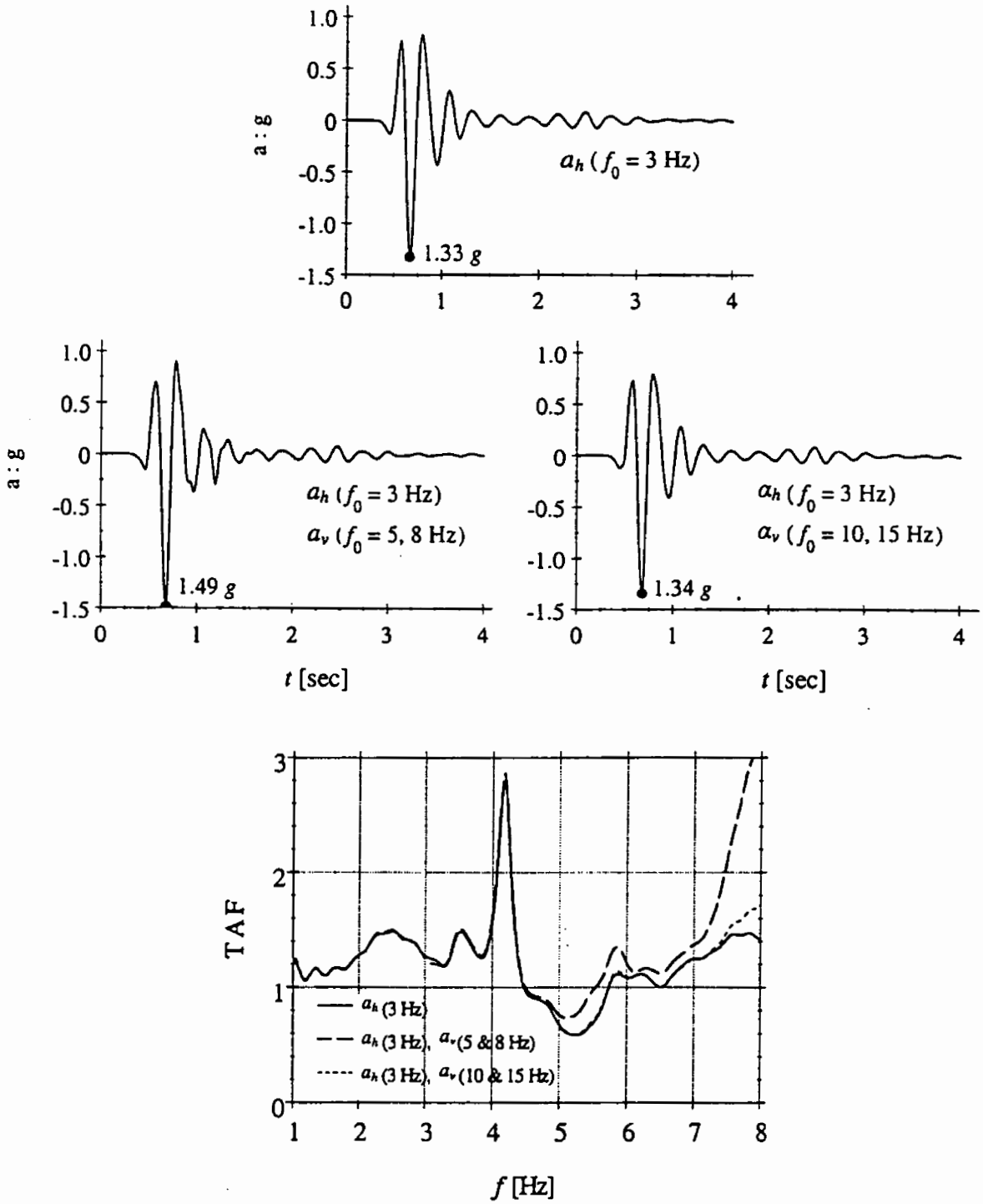

Fig. 20(a). Horizontal acceleration time histories at location (x = 10 m) from the crest and spectrum of the Topographic Aggravation Factor, for a simultaneous SV and P wave excitation: SV wave excitation of a Ricker f_0 = 3 Hz wavelet, P-wave excitations of a double Ricker wavelet f_0 = 5 and 8 Hz and f_0 = 10 and 15 Hz. *Profile A*.

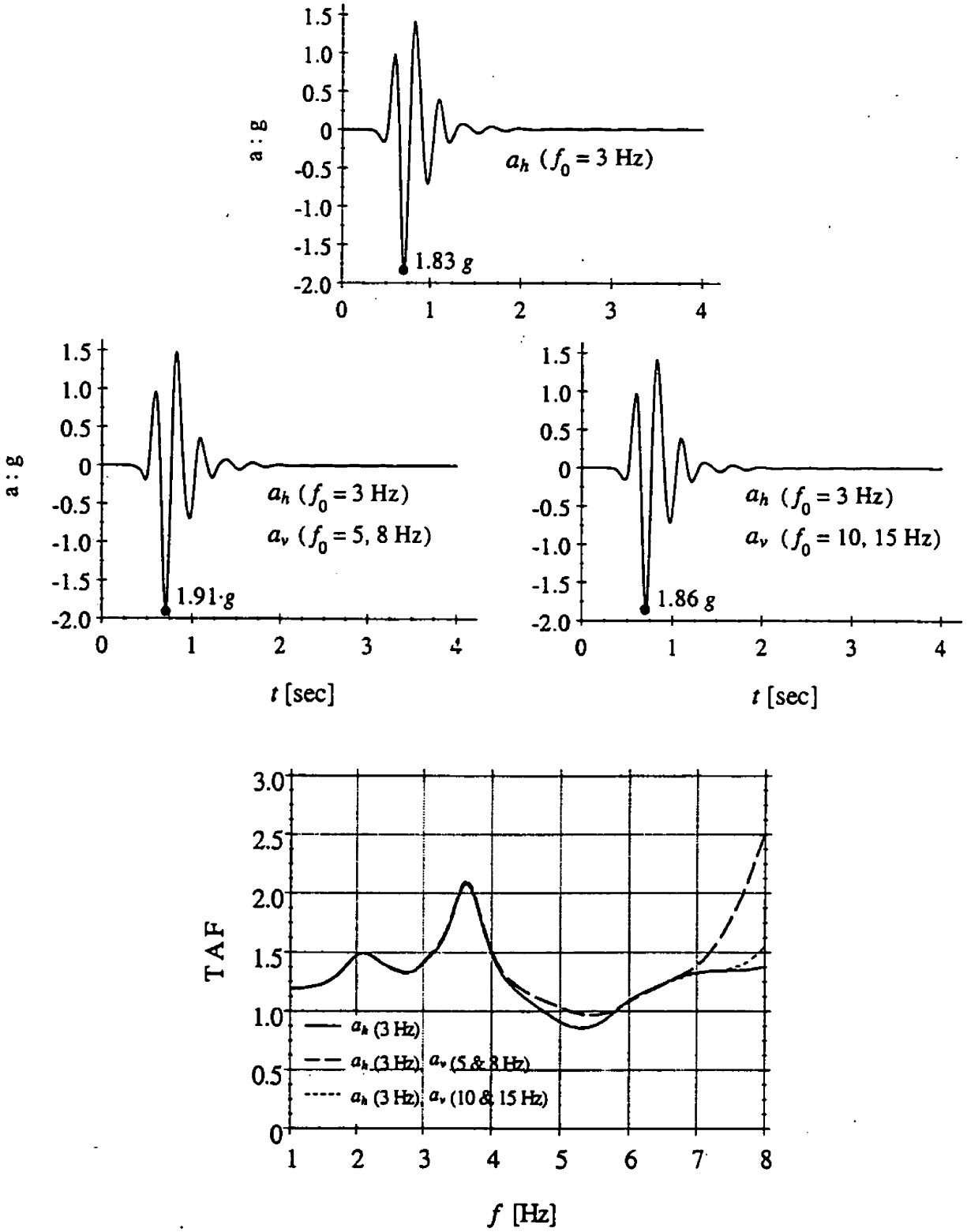

Fig. 20(b). Horizontal acceleration time histories at location (x = 10 m) from the crest and spectrum of the Topographic Aggravation Factor, for a simultaneous SV and P wave excitation: SV wave excitation of a Ricker f_0 = 3 Hz wavelet, P-wave excitations of a double Ricker wavelet f_0 = 5 and 8 Hz and f_0 = 10 and 15 Hz. *Profile B.*

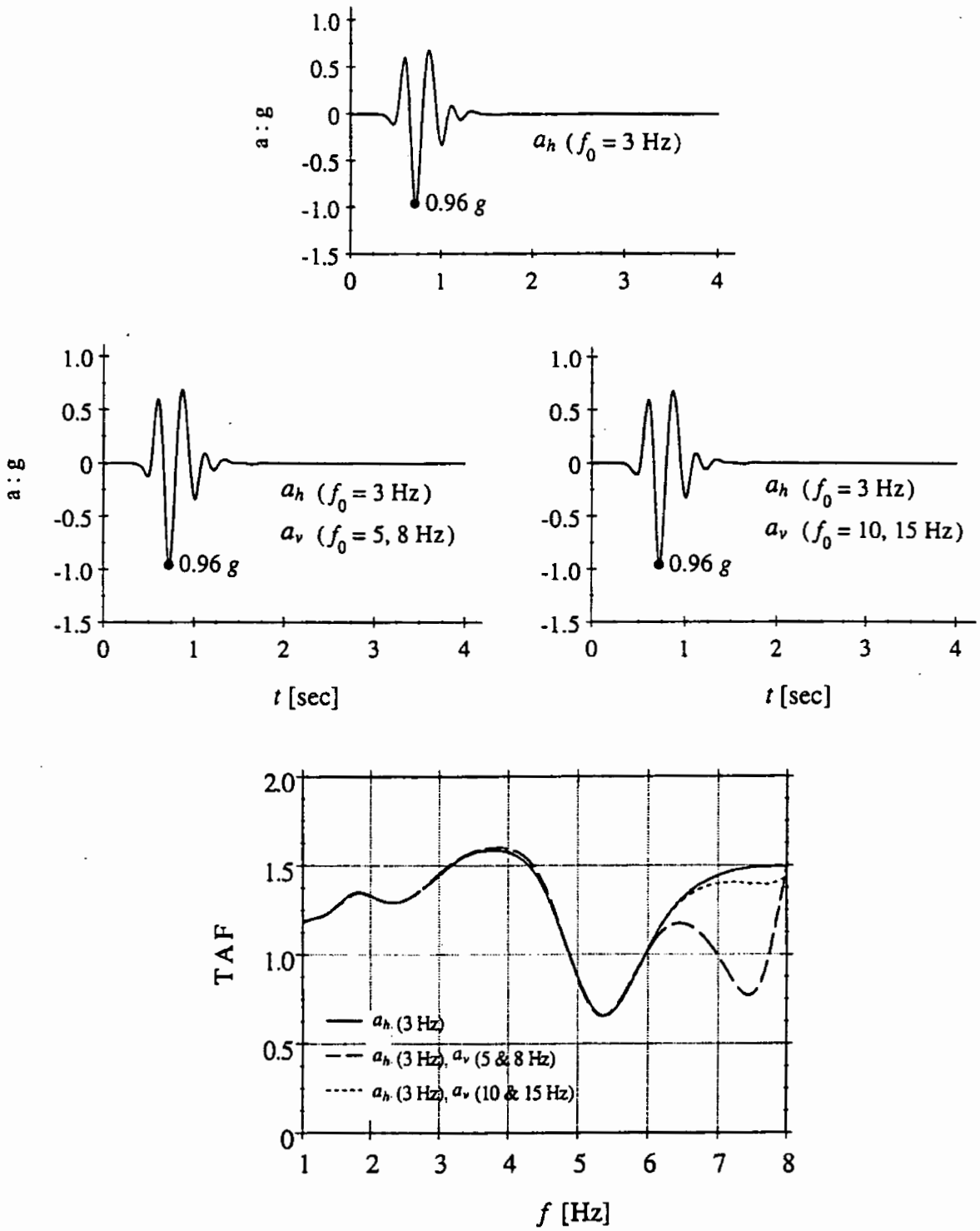

Fig. 20(c). Horizontal acceleration time histories at location (x = 10 m) from the crest and spectrum of the Topographic Aggravation Factor, for a simultaneous SV and P wave excitation: SV wave excitation of a Ricker f_0 = 3 Hz wavelet, P-wave excitations of a double Ricker wavelet f_0 = 5 and 8 Hz and f_0 = 10 and 15 Hz. *Profile C.*

In terms of the spectrum of the Topographic Aggravation Factor for the horizontal component of the response, the configuration with soil characteristics corresponding to Profile A is mainly affected — whilst for Profiles B and C, the effect becomes present in higher frequencies, which however are beyond the range of interest for the present study.

6.3. *Direction of the incident wavefield*

In the present section, the effect of the angle of incidence of an incoming SV Ricker wavelet (with central frequency $f_0 = 3$ Hz) on the observed two-dimensional (topographic) amplification near the crest of the analysed geometry configuration is studied, for the three profiles under investigation.

Based on our analyses, it is believed that the wave-field pattern near the cliff, in the case of a vertically incident SV Ricker wavelet, consists not only of the superposition of direct, reflected/transmitted, diffracted and Rayleigh waves, but also of SP waves generated at the cliff surface due to the critical or near-critical incidence of the vertical SV waves (the angle $i = 30°$ of the slope is $i \approx \vartheta_{cr} \approx \arcsin(V_s/V_p)$, for the realistic value of $v = 0.35$ of the Poisson's ratio adopted for the analyses).

The generation of SP waves in the case of critical incidence of SV waves has been in detail examined by Bard [1982], according to whom, the surface motion at the crest may be amplified by a factor of nearly two in the case of the critical angle incidence.

In an attempt to verify this notion, the configuration portrayed in Fig. 5 (with layered soil structures corresponding to the three Profiles A–C under investigation) is herein subjected to an inclined incident SV Ricker wave-field. The cases studied are schematically shown in Fig. 21 and the spatial distribution of the normalised peak horizontal acceleration is shown in Fig. 22.

As it can be readily seen, two-dimensional amplification is stronger in the case of a vertical (or close to vertical $\vartheta = 15°$) incident wave, practically of the same

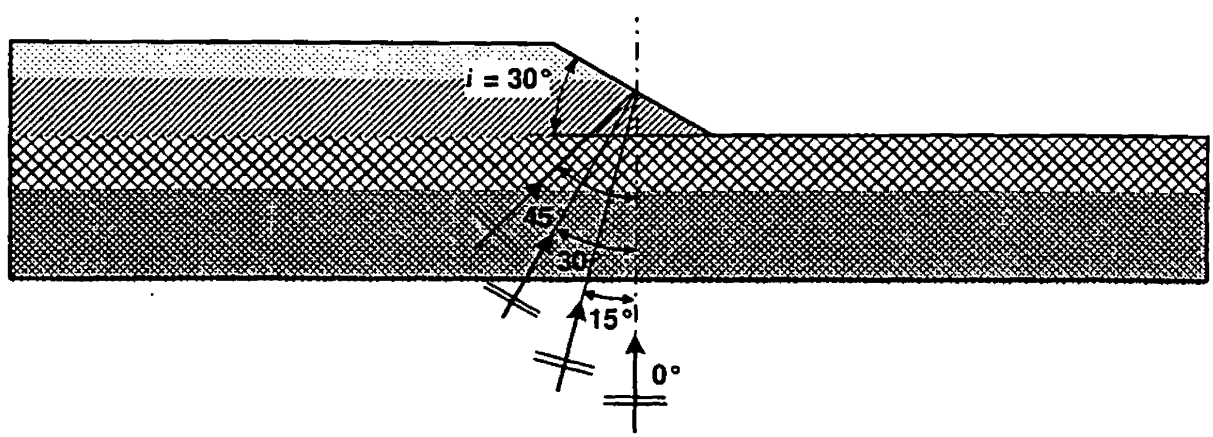

Fig. 21. Schematic representation of the parametric cases to investigate the effect of the angle of wave incidence on the amplification of motion near the crest.

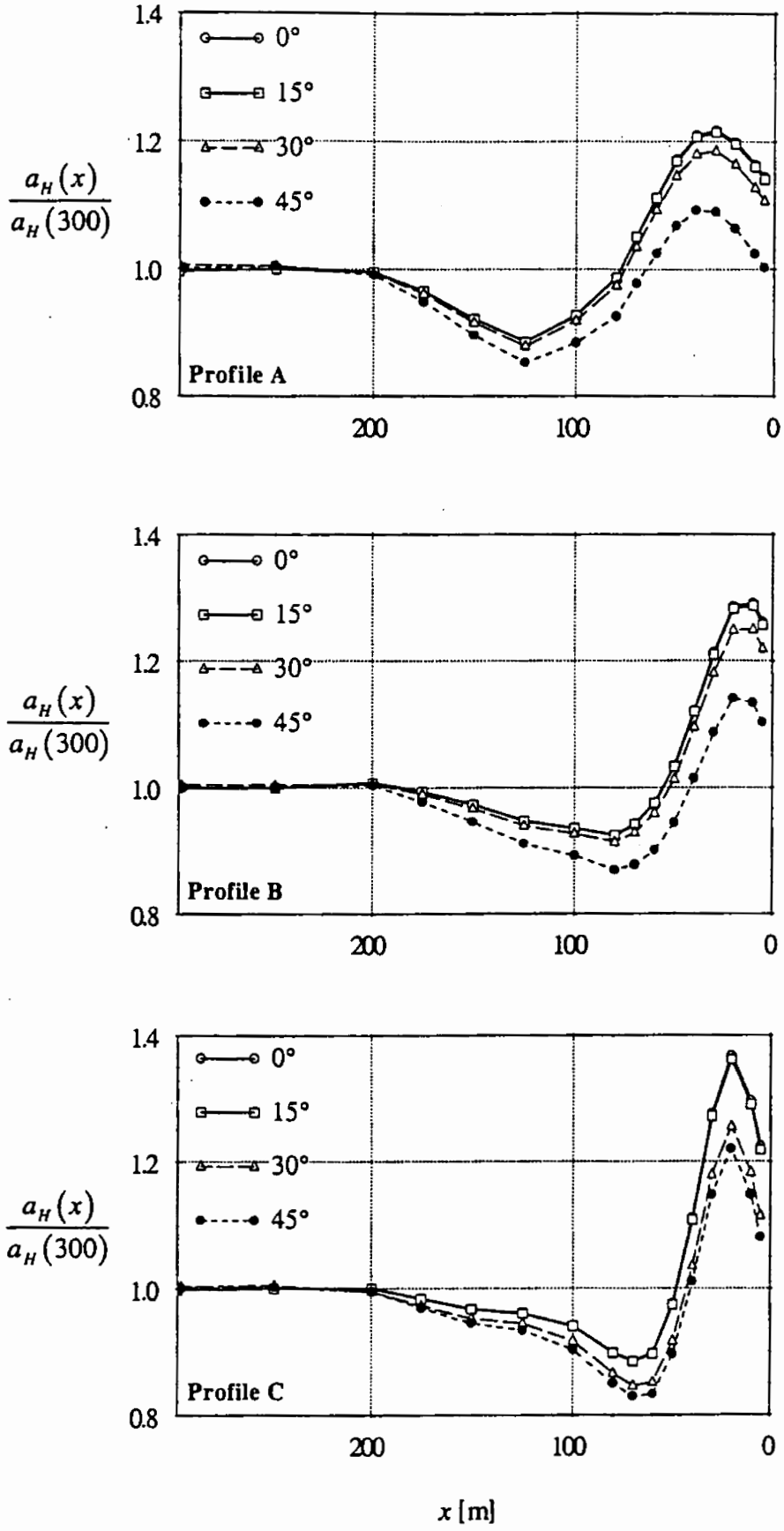

Fig. 22. Effect of the angle of incidence of an SV Ricker wavelet ($f_0 = 3$ Hz) on the distribution of the normalised peak horizontal acceleration, for the three profiles under investigation.

order of magnitude for an angle of incidence of $\vartheta = 30°$, and relatively lower when $\vartheta = 45°$.

In particular, for more-or-less a vertically propagating direct SV wave-field, SP waves are generated at the cliff surface and propagating towards the crest, where the motion is amplified. This is also the case for a wave-field propagating with an angle of incidence of $\vartheta = 30°$ — this time at the horizontal surface on the left of the cliff, where SP waves are again generated and moved to the right towards the crest, resulting again to a large amplitude of the horizontal response when combined with the diffracted wave-field at the topographic irregularity. For the case of $\vartheta = 45°$, such phenomena are not present, resulting in a lower topography amplification in the vicinity of the irregularity and a smoother distribution of the normalised peak horizontal acceleration along the ground surface.

Summarising the results from the site-specific parametric study performed in the present section, it is concluded that in conjunction with soil stratigraphy, the following parameters may play an important role in modulating the surface response near a two-dimensional non-horizontal topography:

- The frequency content of the incident pulse significantly affects the response, producing additional two-dimensional amplification of the motion when resonant frequencies of the one-dimensional soil column are excited. This is true both for the magnitude and the spatial distribution of the surface response. However, the resulting Topography Aggravation Factor spectrum remains practically invariant, as long as the frequency content of the incident motion roughly coincides with the frequency range of interest, a fact which encourages the use of simple broadband pulses — such as the Ricker wavelet used herein — for the study of site effects.
- The simultaneous incidence of SV and high frequency/low amplitude P-waves (characteristic of real earthquake incidents), mainly affects the response of stiff soil profiles — with the magnitude of the *parasitic* horizontal component of the surface motion arising from the incident P-wave — reaching values as high as 45% of the vertical component at the corresponding location. For incident P-waves however, with frequency content beyond the range of interest for seismic problems (> 15 Hz), the effects on the surface response are considered negligible.
- The obliquity of the incident SV waves may play a very significant role in the amplification of the surface motion, for a critical or near-critical incidence, due to the generation of SP surface waves, which interfere with the direct, reflected/transmitted, diffracted, and Rayleigh waves.

7. Recorded Field Evidence

Significant corroboration of the aforementioned theoretical findings comes from two sets of ground motions, recorded during two strong aftershocks. The instruments were installed in the free field, at the locations shown in Fig. 5: two were next to the collapsed factory of FARAN, at location $x \approx 300$ m (near the boreholes B_3 and

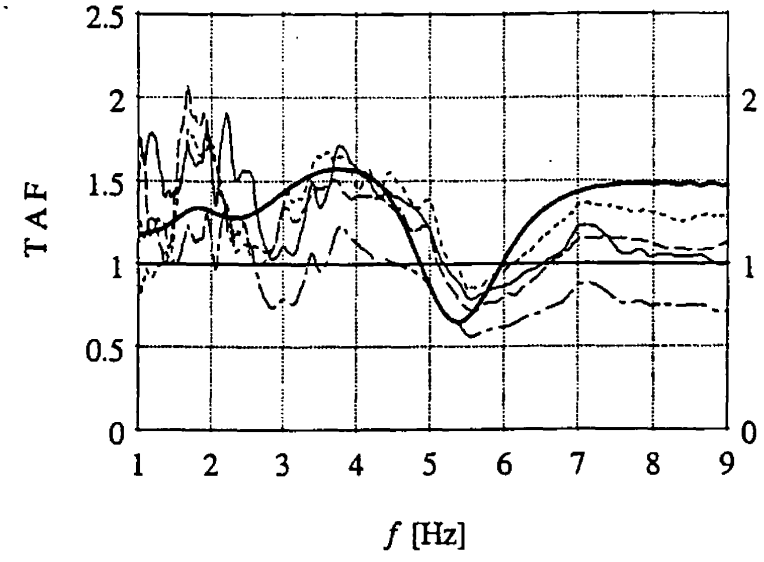

Fig. 23. Spectrum of the Topographic Aggravation Factor obtained as the transfer function between $x = 10$ m and $x = 300$ m from the records of two strong aftershocks, and comparison with numerical results.

B_4), and one in the centre of Site 3 — located at $x \approx 10$ m from the crest, next to borehole B_1. The Site 3 and one of Site 2 seismographs belonged to the University of Athens Seismological Laboratory (courtesy of Professor K. Makropoulos); the second instrument of Site 2 belonged to ITSAK (courtesy of Dr. N. Theodoulidis).

The two major aftershocks have provided the four *empirical* TAF spectra plotted in Fig. 23. It should be noted herein that since Sites 2 and 3 mentioned above, correspond to the soil Profiles B and C respectively, the Fourier spectra evaluated from the aftershock accelerograms have been initially divided by the one-dimensional transfer function for each profile (estimated from the low-strain dynamic soil properties for peak accelerations of the order of 0.015 g). Thus, the variability due to soil-column flexibility effects has been eliminated. To achieve this, the 1D wave propagation analyses, already performed for each horizontally layered profile, were utilised.

Also plotted in Fig. 23 is the numerically computed TAF spectrum for Site 3. It can be readily seen that the recorded and computed results are in reasonable agreement, offering support to the conclusions of the present section, as well as to the use of *strong* aftershocks as a valuable guidance in reconnaissance and microzonation studies.

8. Conclusions

An extensive parametric study has been conducted for the geometry of the cliff of a riverbank, where excessive structural damage was observed during the Athens earthquake of September 1999. The analyses have been performed initially for a homogeneous and a simple two-layer soil configuration. Layering has been shown to play a significant role in the two-dimensional amplification near the crest, due

to the presence of transmitted/reflected waves at the boundaries of the soil layers, in addition to the diffracted wave-field at the topographic irregularity.

Site-specific analyses were then conducted with the selection of soil properties of the layered model based on one-dimensional equivalent linear analyses, thus simulating in a simplified way the nonlinear soil response. In the context of this section, the effect of the frequency content of the selected excitation was investigated by means of the spatial distribution of motion amplification and the spectrum of the "so-called" Topographic Aggravation Factor. The latter is shown to achieve maximal values in the vicinity of the crest, in function of the frequency content of the incident motion, for the geometrical and soil characteristics of a particular topographic configuration.

Two-dimensional amplification due to the presence of a simultaneous P-wave excitation has been also examined, and was proved to be of some significance in certain cases, depending strongly on the frequency content of the selected vertical motion and the soil properties of the analysed profile.

Finally, the effect of the obliquity of the incident wave field has been investigated for the site-specific soil conditions. It has been found that the vertically incident SV waves (mostly assumed in the present study) result in nearly the strongest topographic amplification next to the crest. This, however, may be a geometric coincidence as in this case [slope of 2(H) : 1(V)] the vertical direction nearly coincides with the critical incidence direction, for the soil properties of the analysed configuration.

References

AFPS [1990] *Guidelines for Seismic Microzonation Studies*, AFPS/DRM, 4 pp.

Aki, K. [1988] "Local site effects of ground motion," in *Earthquake Engineering and Soil Dynamics II: Recent Advances in Ground Motion Evaluation*, Von Thun J. L. (editor), Geotechnical Special Publication No. 20, ASCE, New York, 103–155.

Ashford, S. A. and Sitar, N. [1997] Analysis of topographic amplification of inclined shear waves in a steep coastal bluff, *Bull. Seism. Soc. Am.* **87-3**, 692–700.

Ashford, S. A., Sitar, N., Lysmer, J. and Deng, N. [1997] "Topographic effects on the seismic response of steep slopes," *Bull. Seism. Soc. Am.* **87**(3), 701–709.

Bard, P. Y. [1982] "Diffracted waves and displacement field over two-dimensional elevated topographies," *Geophys. J. R. Astr. Soc.* **71**, 731–760.

Bard, P. Y. [1999] "Local effects on strong ground motion: Physical basis and estimation methods in view of microzoning studies," *Proc. Advanced Study Course "Seismotectonic and Microzonation techniques in Earthquake Engineering"*, Kefallinia, Greece, **4**, 127–218.

Bard, P. Y. and Meneroud, J.-P. [1982] "Modification du signal sismique par la topographie Cas de la vallee de la Roya (Alpes-Maritimes)," *Bull. Liaison Laboratoires des Ponts-et-Chausses*, Numero special "Risques Naturels" **150–151**, 140–151.

Boore, D. M. [1972] "A note on the effect of simple topography on seismic SH waves," *Bull. Seism. Soc. Am.* **62**, 275–284.

Boore, D. M., Harmsen, S. C. and Harding, S. T. [1981] "Wave scattering from a step change in surface topography," *Bull. Seism. Soc. Am.* **71-1**, 117–125.

Bouchon, M., Schulz, C. A. and Toksoz, M. N. [1995] "Effect of three-dimensional topography on seismic motion," *J. Geophys. Res.* **101-B3**, 5835–5846.

Bouchon, M. and Barker, J. S. [1996] "Seismic response of a hill: The example of Tanzana, California," *Bull. Seism. Soc. Am.* **86**, 66–72.

Brambati, A., Faccioli, E., Carulli, E. B., Culchi, F., Onofri, R., Stefanini, S. and Ulcigrai, F. [1980] *Studio de microzonizzazione sismica dell'area di Tarcento (Friuli), Edito da Regiona Autonorma Friuli-Venezia Giulia* (in Italian).

Buchbinder, G. G. R. and Haddon, R. A. W. [1990] "Azimuthal anomalies of short-period P-wave arrivals from Nahanni aftershocks, Northwest Territories, Canada, and effects of surface topography," *Bull. Seism. Soc. Am.* **80-5**, 1272–1283.

Casadei, F. and Gabellini, E. [1997] "Implementation of a 3D coupled spectral-element/finite-element solver for wave propagation and soil-structure interaction simulations," *Technical Report*, Joint Research Center, Ispra, Italy.

Castellani, A., Chesi, C., Peano, A. and Sardella, L. [1982] "Seismic response of topographic irregularities," *Proc. International Conference on Soil Dynamics and Earthquake Engineering*, Southampton, 251–268.

Celebi, M. [1987] "Topographical and geological amplifications determined from strong-motion and aftershock records of the 3 March 1985 Chile earthquake," *Bull. Seism. Soc. Am.* **77**, 1147–1157.

Celebi, M. [1995] "Northridge (California) earthquake: Unique ground motions and resulting spectral and site effects," *Proc. 5th Int. Conf. Seismic Zonation*, October 17–19, Nice, France, **11**, 988–995.

Chavez-Garcia, F. J., Sanchez, L. R. and Hatzfeld, D. [1996] "Topographic site effects and HVSR: A comparison between observations and theory," *Bull. Seism. Soc. Am.* **86-5**, 1559–1573.

Earthquake Spectra [2000] 1999 Kocaeli, Turkey, Earthquake Reconnaissance Report: Supplement A to Volume 16, December.

Eurocode 8 [2000] *Design Provisions for Earthquake Resistance of Structures.*

Faccioli, E. [1991] "Seismic amplification in the presence of geologic and topographic irregularities," *Proc. 2nd Int. Conf. Recent Advances in Geotechnical Earthquake Engineering*, St. Louis, II, 1779–1797.

Faccioli, E., Maggio, F., Paolucci, R. and Quarteroni, A. [1997] "2D and 3D elastic wave propagation by a pseudo-spectral domain decomposition method," *J. Seismol.* **1**, 237–251.

Finn, W. and Liam, D. [1991] "Geotechnical engineering aspects of seismic microzonation," *Proc. 4th Int. Conf. Seismic Zonation*, August 25–29, Stanford, California, E.E.R.I. (editor), Oakland CA, **1**, 199–250.

Hibbit, Karlsson, & Sorensen Inc. [1997] ABAQUS.

Housner, G. W. [1990] "Competing against time," *Report to Governor George Deukmejian from the Governor's Board of Inquiry on the 1989 Loma Prieta Earthquake.*

Gazetas, G., Kallou, P. V. and Psarropoulos, P. [2002] "Topography and soil effects in the M_s 5.9 Parnitha (Athens) Earthquake: The case of Adames," *Natural Hazards* **27**, 133–169.

Gazetas, G. [2001] "The 1999 Parnitha (Athens) Earthquake: Soil effects on distribution of damage," *Proc. 15th International Conference on Soil Mechanics and Geotechnical Engineering: Lessons Learned from Recent Strong Earthquakes*, Istanbul, pp. 5–18.

Gazetas, G., Dakoulas, P. and Papageorgiou, A. [1990] "Local-soil and source-mechanism effects in the 1986 Kalamata (Greece) Earthquake," *Int. J. Earthq. Engrg. Struct. Dyn.* **19**, 431–456.

Geli, L., Bard, P. Y. and Jullien, B. [1988] "The effect of topography on earthquake ground motion. A review and new results," *Bull. Seism. Soc. Am.* **78**, 42–63.

Idriss, I. M. and Seed, H. B. [1967] "Response of earthbanks during earthquakes," *J. Soil Mech. Found. Div.*, ASCE, **93**(SM3), 61–82.

Kawase, H. and Aki, K. [1990] "Topography effects at the critical SV wave incidence: Possible explanation of damage pattern by the Whittier-Narrows, California Earthquake of 1st October 1987," *Bull. Seism. Soc. Am.* **80**, 1–22.

Kovacs, W. D., Seed, H. B. and Idriss, I. M. [1971] "Studies of seismic response of clay banks," *J. Soil Mech. Found. Div.*, ASCE, **97**(SM2), 441–455.

LeBrun, B., Hatzfeld, D. and Bard, P. Y. [1999] "Experimental study of ground motion on a large scale topography," *J. Seismol.* **3-1**, 1–15.

Levret, A., Loup, C. and Goula, X. [1986] "The Provence earthquake of June 11th, 1909 (France): New assessment of near-field effects," *Proc. 8th Euro. Conf. Earthq. Engrg.*, Lisbon, September 1986, **2**, 4.2.79.

May, T. W. [1980] "The effectiveness of trenches and scarps in reducing seismic energy," PhD Thesis, University of California at Berkeley, Berkeley, California.

Nechtschein, S., Bard, P. Y., Gariel, J. C., Meneroud, J.-P., Dervin, P., Cushing, M., Gaubert, B., Vidal, S. and Duval, A.-M. [1995] "A topographic effect study in the Nice region," *Proc. 5th Int. Conf. Seismic Zonation*, October 17–19, Nice, France, Ouest Edition Nantes, **11**, 1067–1074.

Ohsaki, Y. [1969] "The effects of local soil conditions upon earthquake damage," *Proc. Specialty Session on Soil Dynamics*, 7th ICSMFE.

Ohtsuki, A. and Harumi, K. [1983] "Effect of topography and subsurface inhomogeneities on seismic SV waves," *Earthq. Engrg. Struct. Dyn.* **11**, 441–462.

Pedersen, H., LeBrun, B., Hatzfeld, D., Campillo, M. and Bard, P. Y. [1994] "Ground motion amplitude across ridges," *Bull. Seism. Soc. Am.* **84**, 1786–1800.

Restrepo, J. I. and Cowan, H. A. [2000] "The 'Eje Cafetero' earthquake, Colombia of January 25 1999," *Bull. New Zea. Soc. of Earthq. Engrg.* **33**, 1–29.

Rogers, A. M., Katz, L. J. and Bennett, T. J. [1974] "Topographic effect on ground motion for incident P-waves: A model study," *Bull. Seism. Soc. Am.* **64**, 437–456.

Rosenblueth, E. [1960] "Earthquake of 28 July 1957 in Mexico City," *Proc. 2nd WCEE* **1**, 359–379.

Sanchez-Sesma, F. J. [1987] "Site effects on strong ground motion," *Soil Dyn. Earthq. Engrg.* **6**(2), 124–132.

Sanchez-Sesma, F. J. [1990] "Elementary solutions for the response of a wedge-shaped medium to incident SH and SV waves," *Bull. Seism. Soc. Am.* **80**, 737–742.

Sanchez-Sesma, F. J., Herrera, I. and Aviles, J. [1982] "A boundary method for elastic wave diffraction: Application to scattering of SH waves by topographic irregularities," *Bull. Seism. Soc. Am.* **72**, 473–490.

Seed, H. B. and Idriss, I. M. [1970] "Soil moduli and damping factors for dynamic response analyses," *Report EERC 70-10*, Earthquake Research Center, University of California, Berkeley.

Seed, H. B., Whitman, R. V., Dezfulian, H., Dobry, R. and Idriss, I. M. [1972] "Soil conditions and damage in the 1967 Caracas Earthquake," *J. Soil Mechanics and Foundations*, ASCE, **98**, 787–806.

Seed, H. B. and Romo, M. P. *et al.* [1987] "Relationships between soil conditions and earthquake ground motions in Mexico City in the earthquake of September 19, 1985," *Report No. EERC-87-15*, University of California, Berkeley.

Sills, L. B. [1978] "Scattering of horizontally-polarised shear waves by surface irregularities," *Geophys. J. R. Astr. Soc.* **54**, 319–348.

Siro, L. [1982] "Southern Italy November 23, 1980 Earthquake," *Proc. 7th Euro. Conf. Earthq. Engrg.*, September 20–25, Athens: Technical Chamber of Greece **7**, 419–429.

Sitar, N. and Clough, G. W. [1983] "Seismic response of steep slopes in cemented soils," *J. Geotechn. Engrg.*, ASCE, **109**, 210–227.

Smith, W. D. [1975] "The application of finite element analysis to body wave propagation problems," *Geophys. J. R. Astr. Soc.* **42**, 747–768.

Soils and Foundations [1996] Special issue on Geotechnical Aspects of the January 17, 1995 Hyogoken-Nambu earthquake, January.

Tezcan, S. S., Yerlici, V. and Durgunoglou, H. T. [1979] "A reconnaissance report for the Romanian earthquake of 4 March 1977," *Engrg. and Struct. Dyn.* **6**, 397–421.

Trifunac, M. D. [1973] "Scattering of plane SH waves by a semi-cylindrical canyon," *Int. J. Earthq. Engrg. Struct. Dyn.* **1**, 267–281.

Tucker, B. E., King, J. L., Hatzfeld, D. and Nersesov, I. L. [1984] "Observations of hard rock site effects," *Bull. Seism. Soc. Am.* **74**, 121–136.

Wong, H. L. and Trifunac, M. D. [1974a] "Scattering of plane SH waves by a semi-elliptical canyon," *Int. J. Earthq. Engrg. Struct. Dyn.* **3**, 157–169.